

<http://hdl.handle.net/###>

# Characterization of ESX-1 components EccA<sub>1</sub>, EspG<sub>1</sub> and EspH reveals differential roles of ESX-1 substrates in the *Mycobacterium marinum* infection cycle

Lisanne M. van Leeuwen<sup>2,a</sup>, Trang H. Phan<sup>1,a</sup>, Coen Kuijl<sup>2</sup>, Roy Ummels<sup>2</sup>, Gunny van Stempvoort<sup>2</sup>, Alba Rubio-Canalejas<sup>1</sup>, Sander R. Piersma<sup>3</sup>, Connie R. Jiménez<sup>3</sup>, Astrid M. van der Sar<sup>2</sup>, Edith N. G. Houben<sup>1</sup>, Wilbert Bitter<sup>1,2</sup>

<sup>1</sup> *Section Molecular Microbiology, Amsterdam Institute of Molecules, Medicines & Systems, Vrije Universiteit Amsterdam, Amsterdam, The Netherlands*

<sup>2</sup> *Department of Medical Microbiology and Infection Control, VU University Medical Center, Amsterdam, the Netherlands*

<sup>3</sup> *Department of Medical Oncology, OncoProteomics Laboratory, VU University Medical Center, Amsterdam, the Netherlands*

<sup>a</sup> *Authors contributed equally*

*Submitted*

## ABSTRACT

The pathogen *Mycobacterium tuberculosis* employs a range of ESX-1 substrates to manipulate the host and build a successful infection. Although the importance of ESX-1 secretion in virulence is well established, the characterization of its individual components and the role of individual substrates is far from complete. Here, we describe the functional characterization of the accessory ESX-1 proteins EccA<sub>1</sub>, EspG<sub>1</sub> and EspH, *i.e.* proteins that are neither substrates nor structural components. Proteomic analysis revealed that EspG<sub>1</sub> is crucial for ESX-1 secretion, since all detectable ESX-1 substrates were absent from the cell surface and culture supernatant in an *espG<sub>1</sub>* mutant. Deletion of *eccA<sub>1</sub>* resulted in minor secretion defects, but interestingly, the severity of these secretion defects was dependent on the culture conditions. Finally, *espH* deletion showed a partial secretion defect, secretion of EspE, EspF was fully blocked whereas secretion of EsxA/EsxB was diminished. Despite the observed differences in secretion, hemolytic activity was lost in all our mutant strains, implying that hemolytic activity is not strictly correlated with EsxA secretion. *In vitro* infection experiments did show significant differences between the mutants, as EspG<sub>1</sub> and EspH, but not EccA<sub>1</sub>, play a major role in early stages of infection. Surprisingly, while EspH is essential for successful infection of phagocytic host cells, deletion of *espH* resulted in a significantly increased virulence phenotype in zebrafish larvae, linked to poor granuloma formation and extracellular outgrowth. Together, these data show different sets of ESX-1 substrates play different roles at various steps of the mycobacterial infection cycle.

## KEYWORDS

ESX-1 secretion; EccA<sub>1</sub>; EspG<sub>1</sub>; EspH; virulence; zebrafish; EsxA, chaperone

## INTRODUCTION

*Mycobacterium tuberculosis*, the etiological agent for the disease tuberculosis (TB), is still one of the most dangerous pathogens for the global health (World Health Organization, 2017). Successful infection requires secretion of multiple virulence factors by *M. tuberculosis*. These virulence factors are exported to the extracellular milieu through the uniquely complex mycobacterial cell envelope. To facilitate this transport, pathogenic mycobacteria have up to five type VII secretion systems (T7SS), called ESX-1 to ESX-5, of which at least three are essential for growth and/or virulence (Abdallah et al., 2007; Gröschel et al., 2016). The ESX-1 locus was the first T7SS to be identified by studying the *Mycobacterium bovis* BCG vaccine strain. The decisive factor in attenuation of this vaccine strain is the Region of Difference 1 (RD1) that deletes part of the ESX-1 locus (Mahairas et al., 1996). Mouse infection experiments utilizing *M. tuberculosis* with a deletion in RD1 showed reduced granuloma formation, the characteristic pathological hallmark of mycobacterial disease (Lewis et al., 2003; Ramakrishnan, 2012), while complementation of the complete RD1 locus in *M. bovis* BCG improved the strain virulence but not comparable with *M. tuberculosis* (Pym et al., 2002). Similarly, efficient granuloma formation, dissemination of disease and invasion of endothelial cells in the fish-pathogen *Mycobacterium marinum* is dependent on a functional ESX-1 secretion system (Gao et al., 2004; Stoop et al., 2011; Volkman et al., 2004; van Leeuwen et al., Chapter 5). More detailed analysis showed that ESX-1 substrates are required for phagosomal membrane rupture (Simeone et al., 2012; van der Wel et al., 2007). The subsequent bacterial accessibility to the cytosol facilitates bacterial survival and intracellular outgrowth, but also triggers innate immune response cascades and defense mechanisms.

Thus far, about a dozen different proteins have been identified that are secreted through ESX-1, which can be divided in three subgroups, the Esx proteins, the PE/PPE proteins and the Esp proteins. Of these substrates, the Esp proteins are ESX-1 specific. The Esx proteins, including the ESX-1 substrates EsxA (ESAT-6) and EsxB (CFP-10), are secreted as antiparallel heterodimers (Renshaw et al., 2005). Interestingly, the limited structural data available for PE and PPE proteins also show that these proteins form a heterodimer (Chen et al., 2017; Korotkova et al., 2014; Strong et al., 2006). These heterodimers are structurally related, as they form a four-helix bundle and contain a YxxxD/E secretion motif directly after the helix-turn-helix on one of the Esx proteins and on the PE protein (M. H. Daleke et al., 2012; Strong et al., 2006). The ESX-1 substrate EspB is probably not secreted as a dimer, but does form a similar four helix bundle with the conserved secretion motif at the same position in the structure (Korotkova et al., 2014; Solomonson et al., 2015).

Of the ESX-1 substrates, EsxA and EsxB are most intensively investigated (Andersen et al., 1995; Hsu et al., 2003; Smith et al., 2008; van der Wel et al., 2007). EsxA is thought

to be responsible for ESX-1 related virulence determinants (De Leon et al., 2012; Hsu et al., 2003; Peng and Sun, 2017; Smith et al., 2008; van der Wel et al., 2007), although this has recently been disputed (Conrad et al., 2017). EspA and EspB have additionally been implicated to be important for virulence (Chen et al., 2013; McLaughlin et al., 2007). However, studying the exact role of each substrate is complicated, as deletion of *esxA/esxB* abolishes secretion of all different Esp proteins (Fortune et al., 2005; Gao et al., 2004), while *espA* and *espB* deletion mutants are unable to secrete EsxA/EsxB (Fortune et al., 2005; McLaughlin et al., 2007).

The ESX-1 secretion system consists of a membrane complex composed of the ESX conserved components (Ecc) EccB<sub>1</sub>, EccCab<sub>1</sub>, EccD<sub>1</sub> and EccE<sub>1</sub> (D. Houben et al., 2012; Van Winden et al., 2016), which is stabilized by the MycP<sub>1</sub> protein (Van Winden et al., 2016). The ESX-1 secretion system additionally contains the cytosolic accessory components EspG<sub>1</sub> and EccA<sub>1</sub>. Homologues of these accessory components are present in some but not all other ESX systems (Houben et al., 2014). The presence of *espG* is linked to the presence of *pe/ppa* genes, which is in line with the observation that EspG functions as a specific chaperone of cognate PE/PPE substrates (Maria H. Daleke et al., 2012; Phan et al., 2017). Deletion of *espG*<sub>1</sub> leads to a block in the secretion of PE35/PPE68\_1 in *M. marinum*, but also of EsxA (Phan et al., 2017). This latter effect is probably indirect, as Esx proteins lack an EspG binding domain. Concomitantly, deletion of *espG*<sub>1</sub> in *M. tuberculosis* caused severe attenuation, both in cell infection and in mice (Bottai et al., 2011). EccA<sub>1</sub> is a cytosolic AAA+ ATPase (ATPases Associated with diverse cellular Activities) and suggested to be involved in a range of diverse processes of secretion (Ates et al., 2016). For example, EccA<sub>1</sub> has been shown to bind to the C terminus of EspC, which is a necessary step for EspC secretion in *M. tuberculosis* (DiGiuseppe Champion et al., 2009). Moreover, EccA proteins of the ESX secretion systems in general have been hypothesized to bind to the PE/PPE-EspG complexes, which would be required for dissociation of the PE/PPE from the chaperone and passing the substrates to the membrane embedded secretion channel (Ekiert and Cox, 2014). This seems logical, as EccA proteins are restricted to ESX systems that also encode EspG, PE and PPE proteins. Virulence studies in zebrafish with *M. marinum* resulted in an attenuated phenotype of an *eccA*<sub>1</sub>-null strain in zebrafish larvae and suggested a functional link between EccA<sub>1</sub> and mycolic acid synthesis (Joshi et al., 2012). However, its exact function is not further characterized.

The genes *espG*<sub>1</sub> and *eccA*<sub>1</sub> are separated in the *esx-1* locus by *espH*. EspH-like proteins are unique for the ESX-1 system. In *M. tuberculosis* there is a single homologue of EspH, which is EspD and has 55% sequence identity. EspD is encoded by the *espACD* locus, located more than 260 kb upstream of the ESX-1 gene cluster. Interestingly, EspD has been shown to be required for the secretion of EsxA, which could be due to its role in stabilizing the intracellular levels of the secreted substrates EspA and EspC (Chen et al.,

2012). These observations suggest that EspH might also be functional as a molecular chaperone.

As several studies have shown the roles of EspG<sub>1</sub> and EccA<sub>1</sub> in the recognition of specific ESX-1 substrates (Maria H. Daleke et al., 2012; Joshi et al., 2012; Phan et al., 2017) and EspH might have a similar role in the recognition of specific Esp proteins, we hypothesized that mutants in these individual ESX-1 accessory genes might have distinctive effects on secretion of different ESX-1 substrates, allowing the analysis of their individual roles in virulence. Here, we reveal that single deletion of *espG<sub>1</sub>*, *eccA<sub>1</sub>* and *espH* in *M. marinum* indeed resulted in distinctive secretion profiles. In accordance with this, the three mutants displayed distinctive and contrasting virulence phenotypes, demonstrating that ESX-1 substrates play different roles in virulence.

## MATERIALS AND METHOD

### Bacterial strains and cell cultures

All *M. marinum* strains that were used in this study were derived from the wild-type strain M<sup>USA</sup> (Abdallah et al., 2006). The *eccCb<sub>1</sub>* (M<sup>VU</sup>) strain was previously identified as an ESX-1 secretion mutant with a spontaneous out of frame mutation in *eccCb<sub>1</sub>* (Abdallah et al., 2009) and also the knock-out strain *espG<sub>1</sub>* was described before (Phan et al., 2017). The knockout strains of *eccA<sub>1</sub>* and *espH* were generated using the mycobacteriophage approach (see below). All strains were routinely cultured on Middlebrook 7H10 plates or in Middlebrook 7H9 medium (Difco) containing ADC supplement or on Sauton medium (Allen, 1998) supplemented with 2% glycerol and 0.015% Tween-80. When required, 0.05% Tween-80 and the appropriate antibiotics were added (25 µg/ml kanamycin (Sigma) and/ or 50 µg/ml hygromycin (Roche)). *M. marinum* cultures and plates were incubated at 30°C. *E. coli* TOP10F' was used for cloning experiments to generate the complemented plasmids and was grown at 37°C on LB plates and in LB medium. Different antibiotics were added to the cultures or plates when necessary at similar concentrations as for *M. marinum* cultures.

### DNA manipulation and plasmid construction

All DNA manipulation procedures followed standard molecular biology protocols. Primers were synthesized and purified by Sigma. Phusion polymerase, restriction enzymes and T4 DNA ligase were obtained from New England Biolabs (NEB). MacroGen performed DNA sequencing.

## RNA Extraction and RT-PCR Analysis

Bacterial RNA was extracted from various *M. marinum* strains as described previously (Phan et al., 2017) and cDNA was synthesized using SuperScript® VILO cDNA Synthesis kit (Thermoscientific) according to manufacturer protocol. For the PCR mix the SYBR® GreenER™ qPCR SuperMix (Thermoscientific) was used according to manufacturer instructions, including the addition of ROX dye reference. qRT-PCR was performed in Applied Biosystems 7500 Fast system. The primer sequences used for qRT-PCR are listed in Table S3. Controls without reverse transcriptase were done on each RNA sample to rule out DNA contamination. The *sigA* gene was used as an internal control.

## Generation of the knockout strains

An *eccA*<sub>1</sub> and *espH* knockout was produced in *M. marinum* M<sup>USA</sup> by allelic exchange using a specialized transducing mycobacteriophage as previously described (Bardarov et al., 1997). High phage titers were prepared following the previously described protocol (Phan et al., 2017). Subsequently, the *M. marinum* wild-type strain was incubated with the corresponding phage to create *eccA*<sub>1</sub> and *espH* knockouts. Colonies that had deleted the endogenous *eccA*<sub>1</sub> and *espH* were selected on hygromycin plates and tested for sucrose sensitivity, induced by the presence of the *sacB* gene. The deletion was confirmed by PCR analysis and sequencing. To remove the resistance and *sacB* gene, a temperature sensitive phage encoding the  $\gamma\delta$ -resolvase (TnpR) (a kind gift from Apoorva Bhatt, University of Birmingham, UK) was used, generating an unmarked deletion mutation. To complement the knockout strain of *espG*<sub>1</sub>, *eccA*<sub>1</sub> and *espH*, the complementing plasmid pMV361::MMAR\_5441/MMAR\_5442/MMAR\_5443 (Km<sup>R</sup>), which was described before (Phan et al., 2017), was used. To clone a region covering *espF*, *espG*<sub>1</sub>, *eccA*<sub>1</sub> and *espH*, the PaeI-HindIII digested fragment of MMAR\_5440/MMAR\_5441/MMAR\_5442/MMAR\_5443 was ligated to the compatible pMV361, resulting in pMV361::*espF/espG*<sub>1</sub>/*espH/eccA*<sub>1</sub> (Km<sup>R</sup>).

## *M. marinum* secretion analysis and immunoblot

*M. marinum* cultures were grown in 7H9 supplemented with ADC and 0.05% Tween 80 until mid-logarithmic phase. Bacteria were washed two times and set to OD<sub>600</sub> of 0.35 in 7H9 medium containing 0.2% glycerol, 0.2% dextrose and 0.05% Tween 80 for overnight growth. Supernatants were filtered using 0.2  $\mu$ m filter, concentrated by trichloric acid (TCA), washed with acetone and the supernatant pellets were resuspended in solubilisation/denaturation (S/D) buffer (containing 100mM DTT and 2% SDS). Bacteria were washed once with PBS. Aliquots were taken for the whole cell lysate preparations and for Genapol X-080 extraction of cell-surface-attached proteins. Bacteria were incubated with 0.5% Genapol X-080 in PBS for 30 minutes with head-over-head rotation at room temperature. Genapol extracted supernatants were denatured in S/D buffer. The bacterial pellet and Genapol extracted cells were lysed by bead beating for 1 minute two

times after which S/D buffer was added. All samples were boiled for 10 minutes at 95°C before loading on SDS-PAGE.

### **Pulldown assays**

For His-tag pulldown, mycobacterial cultures grown to an OD<sub>600</sub> of 1.0 were incubated for 1 h with 100 g/ml ciprofloxacin (Sigma), pellet, washed twice with PBS, and subsequently resuspended in PBS supplemented with Complete protease inhibitor mixture (Roche Applied Science), 1 mM EDTA, and 10 mM imidazole. Cells were broken by two-times passage through a One-Shot cell disrupter (Constant Systems) at 0.83 kbar. Unbroken cells were spun down by repeated centrifugation at 3000 *g*, and subsequently the cell envelope and soluble fractions were separated by ultracentrifugation at 100,000 *g*. Membrane-cleared lysates of *M. marinum* expressing proteins of interest were incubated with Ni-NTA agarose beads (Qiagen) for 1 h at room temperature with head-overhead rotation. After washing the beads five times with phosphate buffer containing 50 mM NaH<sub>2</sub>PO<sub>4</sub> and 300 mM NaCl, (pH 8.0), supplemented with 20 mM imidazole, bound proteins were eluted three times by incubation with phosphate buffer containing 400 mM imidazole. Immunoprecipitation of strep-tagged proteins was performed using the Strep-Tactin® Sepharose® kit (IBA), following the manufacturers protocol.

### **SDS-PAGE, Immunoblotting, and Sera**

Proteins were separated by SDS-PAGE and stained with Coomassie Brilliant Blue G-250 (CBB; Bio-Rad), or transferred to nitrocellulose membranes by Western blotting. The membranes were then incubated with different antibodies followed by enhanced chemiluminescence. Primary antibodies used in this study include: anti- GroEL2 (CS44, Colorado state university), anti-PE\_PGRS antibody (7C4.1F7) (Abdallah et al., 2009), anti-EsxA (Hyb76-8) (Harboe et al., 1998), polyclonal anti-EspE and anti-PPE68 (Carlsson et al., 2009; Pym et al., 2002).

### **LC-MS/MS**

To investigate the cell-surface attached proteome, samples for LC-MS/MS analysis were prepared using the mild detergent Genapol X-080 as previously described (Ates et al., 2015). To prepare the secreted materials, the *M. marinum* M<sup>USA</sup> wild-type and the studied ESX-1 mutant and complemented strains were grown to stationary phase in 7H9 supplemented with ADC, 0.2% glycerol and 0.05% Tween 80. The supernatant fractions containing secreted proteins were collected and spun at 2500 × *g* for an additional 20 min at 4°C and subsequently filtered through a 0.2 μm pore size membrane to remove residual cells and cell debris. The filtered supernatants were 20 times concentrated using 3 kDa molecular weight cut off tubing at 4°C. The retained proteins were TCA precipitated, pelleted, washed in acetone, dried and resuspended in S/D sample buffer

to the corresponding OD of 200 units/ml. All samples were analyzed with SDS-PAGE and CBB staining. Total protein lanes of cell surface and culture supernatant proteins were excised in 3 or 1 fragment(s) per lane, respectively, and analyzed by LC-MS/MS as described before (Ates et al., 2015).

### **Hemolysis assay**

*M. marinum* strains were grown in 7H9 medium supplemented with ADC and 0.05% Tween-80 till the mid-logarithmic phase. All strains were washed once with PBS and inoculated in 7H9 with- or without Tween-80 at 0.35 OD<sub>600</sub>/ml and inoculated for 20 hours. Bacteria were collected by centrifugation, washed once in PBS and diluted in fresh DMEM medium without phenol red (Gibco, Life technologies). Bacteria were quantified by absorbance measurement at OD<sub>600</sub> with an estimation of  $2.5 \times 10^8$  bacteria in 1 ml of 1.0 OD<sub>600</sub>. At the same time, defibrinated sheep erythrocytes (Oxoid-Thermo Fisher, the Netherlands) were washed five times and diluted in the same fresh DMEM medium.  $4.2 \times 10^7$  erythrocytes and  $1 \times 10^8$  bacteria were added for one reaction of 100  $\mu$ l in a round-bottom 96 well-plate, gently centrifuged for 5 minutes and incubated at 32°C. After an incubation of 3 hours, cells were resuspended, centrifuged and 80  $\mu$ l of supernatants were transferred to a flat-bottom 96-wells plate and measured at an absorbance of 405nm to quantify hemoglobin release.

### **Host cell growth conditions**

The mouse macrophage line RAW264.7 (American Type Culture Collection) was cultured in RPMI 1640 with Glutamax-1 (Gibco) supplemented with 10% fetal bovine serum (FBS; Gibco), 100 U of penicillin/ml, 100  $\mu$ g of streptomycin/ml at 37°C, 5% CO<sub>2</sub>. A total of  $3 \times 10^7$  cells was seeded in T175 flasks (Corning). *Acanthamoeba castellanii* was seeded in T175 flasks and grown in PYG medium, which is 0.4M MgSO<sub>4</sub>·7H<sub>2</sub>O, 0.05M CaCl<sub>2</sub>, 0.1 M Sodium citrate·2H<sub>2</sub>O, 0.05M Fe(NH<sub>4</sub>)<sub>2</sub>(SO<sub>4</sub>)<sub>2</sub>·6H<sub>2</sub>O, 0.25M Na<sub>2</sub>HPO<sub>4</sub>·7H<sub>2</sub>O, 0.25M KH<sub>2</sub>PO<sub>4</sub> in distilled water with 2% proteose peptone (W/V, BD 211684) and 0.01% yeast extract. After pH adjustment to 6.5, 2M glucose was added.

### **Host cell infection procedure**

All bacterial strains were grown until the exponential growth phase, washed with 0.05% Tween 80, spun down and resuspended in RPMI medium. RAW macrophages were infected with a MOI of 5 for 3 hours and incubated at 30°C, 5% CO<sub>2</sub>. Cells were washed in RPMI to remove extracellular mycobacteria and either analyzed immediately or incubated for another 21 hours at 30°C, 5% CO<sub>2</sub>. *A. castellanii* (ATCC 30234) infection was performed with a MOI of 1, 3, 9, 27, 54, and 108 to determine optimum MOI, for the remaining experiments MOI 3 was chosen. Incubation for 3 hours or 24 hours was done at 30°C, 5% CO<sub>2</sub>.

## Flow cytometry

Uptake of strains in host cells was quantified for all cell lines with a BD Accuri C6 flow cytometer (BD Biosciences) with a 488-nm laser and 585/40-nm filter to detect mEos3.1. A minimum of 5000-gated events was collected per sample per time point, percentage of living cells, percentage of infected cells and median fluorescent intensity per cell was analyzed using BD CFlow software.

## Injection stocks for zebrafish infection

Injection stocks were prepared by growing bacteria until the logarithmic phase ( $OD_{600}$  of 0.7-1). Bacteria were spun down at low speed for 1 min to remove the largest clumps, washed with 0.3% Tween-80 in phosphate buffered saline (PBS) and sonicated shortly for declumping. Bacteria were then resuspended in PBS with 20% glycerol and 2% PVP and stored at  $-80^{\circ}\text{C}$ . Before use, bacteria were resuspended in PBS containing 0.17% (V/V) phenol red (Sigma) to aid visualization of the injection process.

## Zebrafish infection procedure

Transparent casper zebrafish larvae (White et al., 2008) were removed from their chorion with tweezers and infected at 1 day post fertilization (dpf) via the caudal vein with bacterial suspension containing 50-200 CFU. Injection was performed as described previously (Benard et al., 2012). To determine the exact number of bacteria injected, the injection volume was plated on 7H10 plates containing the proper antibiotic selection. At 4 days post infection (dpi) larvae were analyzed with a Leica MZ16FA fluorescence microscope. Bright field and fluorescence images were generated with a Leica DFC420C camera. Infection levels were quantified with a custom-made fluorescent pixel counting software. The software is in house developed and freely available under MIT license. Following analysis, larvae were fixed overnight in 0.4% (V/V) paraformaldehyde (EMS, 100122) in PBS, washed and stored in PBS for immunohistochemistry.

## Ethics statement

All procedures involving *Danio rerio* (zebrafish) larvae were performed in compliance with local animal welfare laws and maintained according to standard protocols (zfin.org). The breeding of adult fish was approved by the institutional animal welfare committee (Animal Experimental licensing Committee, DEC) of the VU University medical center. All protocols adhered to the international guidelines specified by the EU Animal Protection Directive 86/609/EEC, which allows zebrafish embryos to be used up to the moment of free-living (approximately 5–7 days after fertilization). This work is allowed by the institutional animal welfare committee (Animal Experimental licensing Committee, DEC) of VU/VUmc under project license number MMI10-02,

### **Immunohistochemical stain**

Larvae were rinsed with 1% PBTx, (1% Triton X-100 in PBS), permeated in 0.24% trypsin in PBS and blocked for 3 hours in block buffer (10% normal goat serum (NGS) in 1% PBTx). Samples were incubated with anti-L-plastin [1:500 (V/V) dilution] in antibody buffer (PBTx containing 1% (V/V) NGS and 1% (W/V) BSA) overnight at RT. Samples were washed with PBTx, incubated for 1 hour in block buffer and stained with an Alexa-Fluor-647 goat-anti-rabbit antibody (Invitrogen A21070, 1:400), overnight at 4°C.

### **Confocal microscopy**

Confocal analysis was performed on larvae, embedded in 1% low melting-point agarose (Boehringer Mannheim, 12841221-01) in an 8-well microscopy  $\mu$ -slide (ibidi), Analysis was performed with a confocal laser scanning microscope (Leica TCS SP8 X Confocal Microscope). Leica Application Suite X software and ImageJ software were used to adjust brightness and contrast and to create overlay images and 3D models.

### **Graphs and statistical analysis**

Graphs were made using Graph Pad Prism 6.0. Pixel counts were logarithmic transformed; error bars represent mean and standard error of the mean. A one-way ANOVA was performed followed by a Bonferroni's multiple comparison test to analyze statistical significance. Graphs with results of RAW264.7 and *A. castellanii* infection experiments show percentage-infected cells of total cells; error bars represent mean and standard error of the mean. Data representing the fold change between 3 and 24 hpi was logarithmic transformed. A two-way ANOVA followed by a Sidak's multiple comparison test was performed for statistical significance.

## **RESULTS**

### **Individual ESX-1 components EspG<sub>1</sub>, EspH and EccA<sub>1</sub>, display distinctive effects on the secretion of ESX-1 dependent substrates**

To study the role of accessory ESX-1 proteins EspG<sub>1</sub>, EccA<sub>1</sub>, and EspH in secretion, we created targeted knocked-out strains for *espH* and *eccA<sub>1</sub>*, and used the previously described *espG<sub>1</sub>* knockout in *M. marinum* (Phan et al., 2017). Deletion of the individual genes had no effect on bacterial growth in rich medium (Figure S1A). In addition, qRT-PCR on total RNA extractions showed that the different deletions had no polar effect on the transcription of neighboring genes (Figure S1B).

Next, secretion analysis was performed using immunoblotting and a set of antibodies directed against known ESX-1 substrates. GroEL2 was included as a loading and lysis control. As a known ESX-1 negative mutant we included the M<sup>vu</sup> strain, which has a

frameshift mutation in *eccCb<sub>1</sub>* (Abdallah et al., 2009) (Figure 1B, lane 6 and lane 7, respectively). Our analysis showed that EsxA was no longer secreted in the  $\Delta$ *espG<sub>1</sub>* strain (Figure 1B, lane 9), similarly as observed in a previous study from our group (Phan et al., 2017). Interestingly, the deletion of *espH* also resulted in a dramatic decrease in the secretion of EsxA (Figure 1B, lane 10). Surprisingly, and in contrast to what has been published previously (Gao et al., 2004; Joshi et al., 2012), we observed that secretion of EsxA was reduced in the *eccA<sub>1</sub>* mutant, but not completely aborted (Figure 1B, lane 8).

Next, we analyzed another ESX-1 substrate EspE, a highly abundant cell surface protein of *M. marinum*, which can be extracted from the cell surface using the mild detergent Genapol X-080 (Sani et al., 2010). The surface localization of the ESX-5 dependent PE\_PGRS proteins was included as controls. In the WT strain, EspE was secreted in two forms: a full-length protein of ~ 40 kDa and a putatively processed form of ~ 25 kDa (Figure 1C, lane 6). Surface localization of EspE was abolished in all the tested mutant strains (Figure 1C, lane 7 to lane 10). Notably, while EspE accumulated in the cell pellet of all other strains, this protein was not detected in the pellet fraction of the *espH* mutant (Figure 1C, lane 5), indicating that secretion of EspE was blocked at a different stage as compared to the other mutants.

To confirm that the observed secretion defects were caused by the targeted mutations, complementation plasmids were constructed. Complementation of the *espG<sub>1</sub>* mutant strain could only be achieved when *espF*, the gene upstream of *espG<sub>1</sub>*, was included. Similar results were observed previously for *M. tuberculosis* (Bottai et al., 2011). Two versions of pMV361 complementation plasmid were constructed: the first one includes the genomic region from *espF* (*MMAR\_5440*) to *eccA<sub>1</sub>* (*MMAR\_5443*), whereas in the second plasmid only the *espG<sub>1</sub>-espH-eccA<sub>1</sub>* locus was present. Complementation of the knockout strains with either of these plasmids fully restored the secretion of EsxA and EspE in all of the mutants (Figure 1D and 1E).

### **The absence of *eccA<sub>1</sub>* causes a loss of EsxA secretion under specific conditions**

A major discrepancy with previous publications was our finding that *EccA<sub>1</sub>* has a limited effect on EsxA secretion. Previously, Gao *et al.* showed, using the same *M. marinum* background strain, that *EccA<sub>1</sub>* is crucial for ESX-1 secretion (Gao et al., 2004; Joshi et al., 2012). We realized that there is a difference in the growth conditions used in the two studies; we used 7H9 medium whereas Gao *et al.* used Sauton medium (Gao et al., 2004; Joshi et al., 2012). To test whether the observed differences could be linked to a difference in growth condition, secretion analysis was performed on cultures grown in Sauton medium. Interestingly, whereas the results for  $\Delta$ *espG<sub>1</sub>* and  $\Delta$ *espH* were identical to the previous experiment using 7H9 medium (Figure 2, lane 9 and lane 10, respectively), EsxA was no longer secreted in the *eccA<sub>1</sub>* mutant strain (Figure 2, lane 8). Together, these results suggest that the role of *EccA<sub>1</sub>* in the secretion of EsxA is dependent on the growth condition.

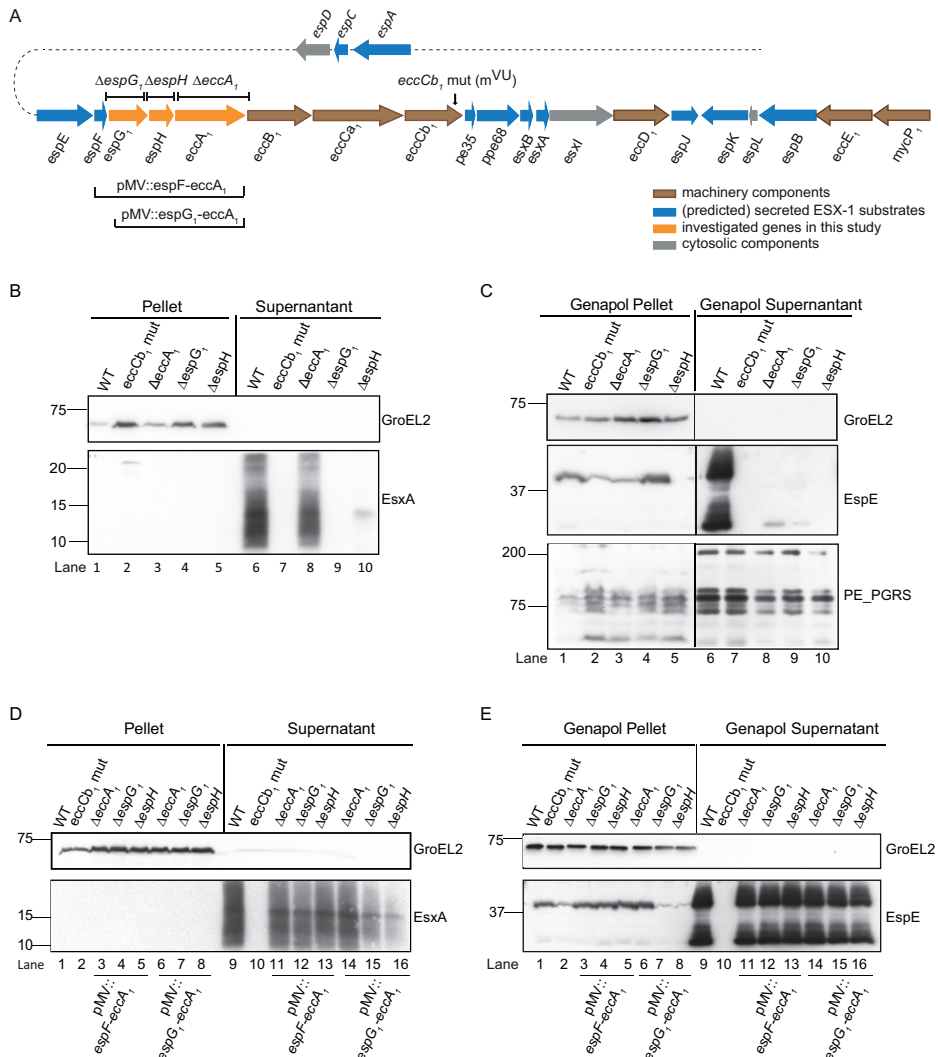


**Figure 1. Mutants affected in the ESX-1 accessory proteins EspG<sub>1</sub>, EspH and EccA<sub>1</sub> differently affect the ESX-1 secretome.**

[A] Genetic organization of *espG<sub>1</sub>-espH-eccA<sub>1</sub>* in the *esx-1* locus. Genes are color-coded according to the localization of their proteins—see key. [B, C] Secretion analysis of EsxA and EspE substrates reveal that single deletion of *espG<sub>1</sub>*, *espH* and *eccA<sub>1</sub>* affects secretion at different levels. Immunoblot analysis using protein preparations of wild-type *M. marinum* and the indicated mutants. In B we analyzed cell pellets not treated with detergent Genapol X-080 and culture supernatant fractions. In C we analyzed cell pellets treated with Genapol X-080 and the concomitant supernatant fractions. [D, E] Complementation of the mutant strains fully restores ESX-1 secretion. In D the secretion of EsxA was analyzed and in E the secretion of EspE. In both experiments, GroEL2 was used as loading control and PE\_PGRS as cell-surface control fraction. Equivalent OD units were loaded; 0.2 OD for pellet or Genapol pellet and 0.5 OD for supernatant or Genapol supernatant fractions.

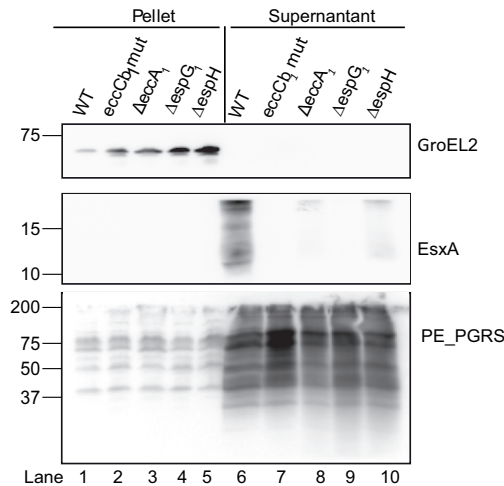


**Figure 2. Secretion of EsxA by the *eccA*, mutant is growth-medium dependent**

Secretion analysis of the WT *M. marinum* M<sup>USA</sup>, the *eccCb*<sub>1</sub> mutant and the knockout strains *espG*<sub>1</sub>, *espH* and *eccA*<sub>1</sub>, grown in Sauton's defined medium. Immunoblot analysis with anti-EsxA confirmed a requirement of EccA, for a full secretion of EsxA when cells were grown in this medium. Anti-GroEL2 was used as a loading and lysis control for all samples. Anti-PGRS antibodies, staining the ESX-5 dependent substrates PE\_PGRS proteins, were used as a supernatant control for all samples. Equivalent OD units were loaded; 0.3 OD for pellet and 0.6 OD for supernatant or supernatant fractions.

### Secretome analysis of accessory ESX-1 protein mutants by LC-MS/MS

The proteome of a number of ESX-1 targeted knockout strains has been determined previously (Champion et al., 2014). However, this study did not include an *espH* mutant and the cell surface proteome was not analyzed. In order to obtain a comprehensive and detailed view, the complete secretome of our mutant strains was analyzed by mass spectrometry. As some ESX-1 substrates are efficiently secreted into the culture supernatant, while others mainly remain attached to the cell surface (Sani et al., 2010), we performed two separate experiments to study the proteome profiles of both cell surface- and secreted proteins. For this, the WT, *eccCb*<sub>1</sub> mutant, *ΔespG*<sub>1</sub>, *ΔespH* and *ΔeccA*<sub>1</sub> and corresponding complemented strains were grown in liquid 7H9 medium with or without Tween 80 to study secreted proteins in the medium or cell surface proteins, respectively. Secreted proteins were separated from bacterial cells by centrifugation and filtering, while cell surface proteins were extracted from the bacterial cells using Genapol X-080. Protein samples from two independent experiments were analyzed by LC-MS/MS and spectral counts were used to measure relative protein abundance across different strains and fractions.

For the *eccCb*<sub>1</sub> mutant, a massive reduction in the secretion of all known ESX-1 substrates, i.e. EsxA, EsxB<sub>1</sub>, EspB, EspC, EspE, EspF, EspJ, EspK and PPE68, was observed, both in the cell surface-enriched fractions (Figure 3A) and the culture supernatants

(Figure 4A). These results are in line with published data (Champion et al., 2014). Also the secretion of several other proteins, including the PE protein MMAR\_2894 and PPE protein MMAR\_5417, was blocked, suggesting they are novel ESX-1 substrates. This notion is strengthened by the fact that these two proteins are homologous to the PE and PPE protein encoded by the *esx-1* locus. For the other proteins that showed reduced spectral counts in the cell surface fractions it is more difficult to draw any conclusion. First of all, the difference in secretion levels are smaller as compared to the known ESX-1 substrates (Figure 3), but furthermore they lack known characteristics of T7S substrates, such as the YxxxD/E secretion motif preceded by a predicted helix-turn-helix structure. The *espG<sub>1</sub>* mutant showed similar secretion profiles as the *eccCb<sub>1</sub>* mutant (Figure 3B and Figure 4B), although the secretion of EspB, EspK and EspE seemed to be slightly less severely affected. This suggests that EspG<sub>1</sub> is not only required as a chaperone for its cognate PE/PPE substrates, but plays a more central role in the secretion of all ESX-1 substrates. The secretion of all ESX-1 substrates returned to the WT levels in the *espG<sub>1</sub>* mutant carrying the pMV361::*espF-eccA<sub>1</sub>* complementation plasmid (Figure S2, A and B).

As expected from the immunoblot analysis, the deletion of *espH* resulted in a severe reduction of EspE and EspF (Figure 3C). This reduction was in fact almost complete, both in the fraction of the surface proteins and in the bacterial pellet, which again suggests instability of intracellular EspE/EspF in the absence of EspH. This effect was restored when the complementation plasmid was introduced (Figure S2, C and D). Interestingly, the effects of the *espH* removal on secretion of EsxA and EsxB<sub>1</sub> was only mildly reduced as compared to the effects in the *eccCb<sub>1</sub>* mutant, while the effects on other ESX-1 substrates, such as EspB, EspK and EspJ were only minor (Figure 4C). This indicates there is no substrate dependency between EspE/EspF and other Esp proteins.

The secretome profiles of the *eccA<sub>1</sub>* mutant on 7H9 medium showed only a mild reduction of ESX-1 substrates in both cell surface and supernatant fractions (Figure 3D and Figure 4D). For instance, EsxA and EsxB<sub>1</sub> secretion was five and two-fold decreased, respectively, while in the *eccCb<sub>1</sub>* mutant the reduction of both was 10 fold (Figure 4D and Table 3). The substrates EspE, EspF, EspJ and EspK are more affected by the *eccA<sub>1</sub>* mutation than the other substrates in both protein fractions. In concordance with the data obtained by immunoblotting, the complementation of the *eccA<sub>1</sub>* mutant with pMV361::*espF-eccA<sub>1</sub>* plasmid restored the secretion of all ESX-1 substrates (Figure S2, E and F).

Surprisingly, we also identified some proteins that were present in significantly increased amounts in the cell envelope fractions of various mutants. One of these proteins is SecA2, a cytosolic component of Sec transport system and proposed to contribute to the virulence of *M. tuberculosis* and *M. marinum* (Braunstein et al., 2003; van der Woude et al., 2013). SecA2 was present in higher amounts in all mutants except the *DespH*, suggesting a link with intracellular accumulation of EspEF. Another intriguing observation is an increase of Mak in the  $\Delta$ *espG<sub>1</sub>*,  $\Delta$ *espH* and the  $\Delta$ *eccA<sub>1</sub>* (Figure 3B, C and D, respectively).

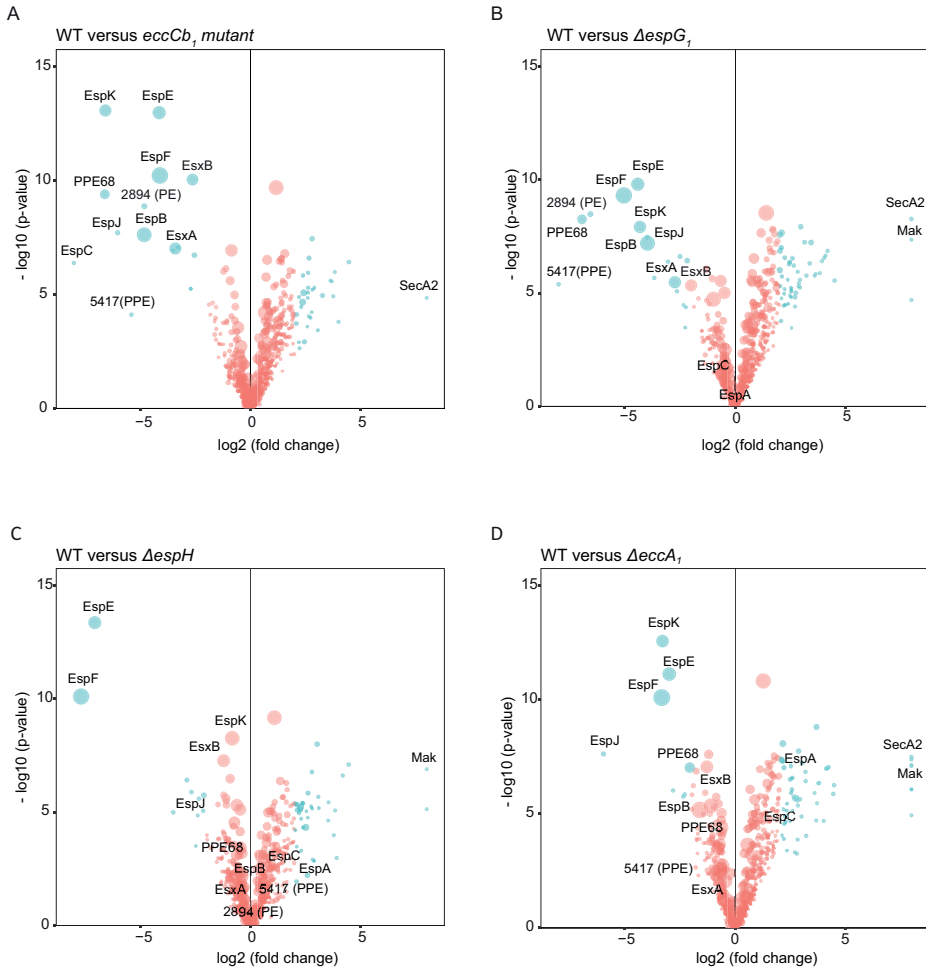


**Figure 3. Quantitative proteomics analysis of the Genapol-enriched fractions of different *M. marinum* ESX-1 mutant strains.**

Volcano plots representing the statistical significance of changes of cell-surface enriched proteins between the WT *M. marinum* and each ESX-1 mutant. The vertical lines depict log base 2 of the p-value and the horizontal lines denote fold change on the  $-\log$  base 10 scale. Only proteins with an accumulative number of more than 10 spectral counts are shown. Each dot corresponds to a single identified protein and the size of the dots correlates to the accumulative spectral counts of the protein of the WT and the corresponding mutant. Proteins with a spectral count difference of more than eight folds were set to eight. In blue: proteins that showed more than 4 folds of change, otherwise in red. Only putative ESX-1 substrates, SecA2 and Mak are annotated. [A] WT versus the *eccCb*, mutant. [B] WT versus the  $\Delta$ *espG*, mutant. [C] WT versus the  $\Delta$ *espH* mutant. [D] WT versus the  $\Delta$ *eccA*<sub>1</sub> mutant.

Mak is a mycobacterial maltokinase whose function is involved in the glycan synthesis from trehalose (Fraga et al., 2015) and considered to be essential for the growth of *M. tuberculosis* (Griffin et al., 2011). This could suggest that there is an indirect effect on the synthesis of ESX-1 secretion on the mycobacterial capsule.

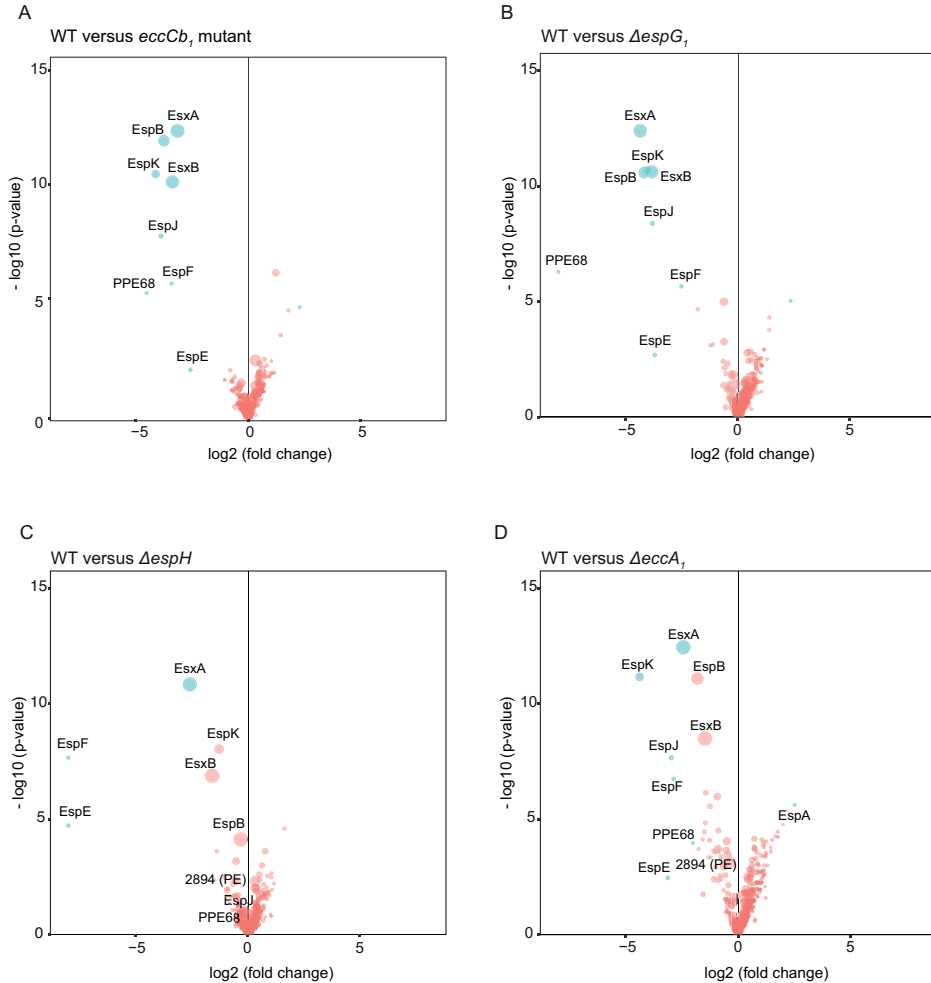


**Figure 4. Quantitative proteomics analysis of the supernatant of different *M. marinum* ESX-1 mutant strains.**

Volcano plots representing the statistical significance of changes of the secreted proteins in the supernatant between the WT *M. marinum* and each ESX-1 mutant. The same quantitative method was used as in Fig. 3 for the Genapol-enriched fractions. [A] WT versus the *eccCb*<sub>1</sub> mutant. [B] WT versus the  $\Delta$ *espG*<sub>1</sub> mutant. [C] WT versus the  $\Delta$ *espH* mutant. [D] WT versus the  $\Delta$ *eccA*<sub>1</sub> mutant.

### EspE specifically interacts with EspH in *M. marinum*

The observation that EspH mainly affects the secretion of EspE/EspF and that EspE could not be detected in the *espH* mutant pellet fraction raised the hypothesis that EspH could either regulate the transcription of *espE/espF* or stabilize EspE/EspF at the protein level. We first tested the effect of *espH* deletion on *espE* mRNA levels. Total mRNA was extracted from the WT *M*<sup>USA</sup>, *eccCb*<sub>1</sub> mutant and  $\Delta$ *espH* strains and qRT-PCR was performed using primer sets for *espE*, *espF* and *esxA*. The results showed that the mRNA levels of all three

genes were comparable in the *eccCb<sub>1</sub>* mutant strains analyzed (Figure S3A). Thus, we could disprove the possibility that EspH regulates *espE* at the transcriptional level. Next, we studied a direct interaction of EspH with EspE and/or EspF. Based on the high homology of EspE with EspA and EspF with EspC, we speculated that EspF might be secreted together with EspE. We therefore constructed a pSMT3 plasmid containing *espE/espF* in which *espE* was modified to express a C-terminal Strep tag. We also introduced a His tag at the C terminus of EspH using the *espG<sub>1</sub>/espH/eccA<sub>1</sub>* complementation plasmid. Introduction of both plasmids in WT and in the  $\Delta$ *espH* mutant resulted in surface localized EspE, as judged by immunoblot analysis of the cell surface extracted protein preparations (Figure S3B). These results show that the addition of the Strep tag to the C terminus of EspE and the His-tag to EspH did not affect the functionality of these proteins in the secretion process.

To study the interaction of EspE and EspH, we overexpressed EspE-Strep/EspF and EspH-His in the *eccCb<sub>1</sub>* mutant strain. The ESX-1 secretion system is defective in this strain and therefore EspE and EspH accumulate in the cytosol, which allows their analysis and co-purification. The subcellular localization of EspE and EspH was examined by a subcellular fractionation procedure, showing that EspE-Strep was partially soluble while EspH-His was exclusively present in the soluble fraction (Figure S3C). Next, we employed the ability of StrepTactin beads to purify Strep-tagged EspE from these soluble fractions. Immunoblot analysis showed that EspE-Strep was efficiently purified using this procedure. Importantly, EspH-His, appearing as a ~ 25 kDa band, was only present in the elution fractions when expressed in the presence of EspE-Strep (Figure 5A). In contrast, the ESX-1 substrates PPE68 and EsxA were not co-purified and both remained in the flow-through fraction.

To confirm this EspE-EspH interaction, a Ni-NTA pull-down assay was performed using lysates of the *eccCb<sub>1</sub>* mutant containing EspE-strep/EspF only or EspE-strep/EspF and EspH-His. Immunoblot analysis using anti-His tag confirmed the efficient purification of EspH-His. Using anti-EspE on these samples showed co-elution of endogenous EspE only in the presence of the His-tagged EspH (Figure 5B). The ESX-1 substrates PPE68 and EsxA were again only found in the flow-through fraction, indicating that they do not bind EspH. In conclusion, these data confirmed our hypothesis that EspH specifically interacts with EspE in the cytosol of *M. marinum* and this interaction is essential for secretion.

### **Effect of accessory ESX-1 proteins on hemolysis**

ESX-1 functioning in *M. marinum* has been associated with lysis of red blood cells (Gao et al., 2004). Because of this, the hemolysis assay has been employed as a model for the ESX-1-dependent lysis of (phagosomal) membranes (Gao et al., 2004). Prior work suggested that the ESX-1–membrane lytic activity was mediated by EsxA through its pore-forming activity (Hsu et al., 2003; Refai et al., 2015). Because the deletion of *espG<sub>1</sub>*,

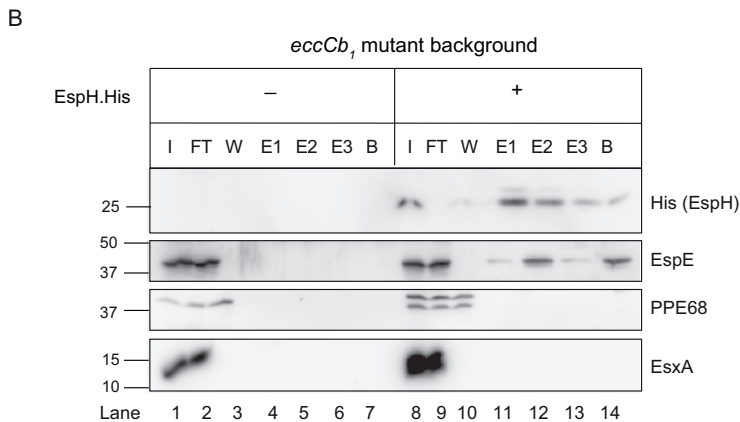
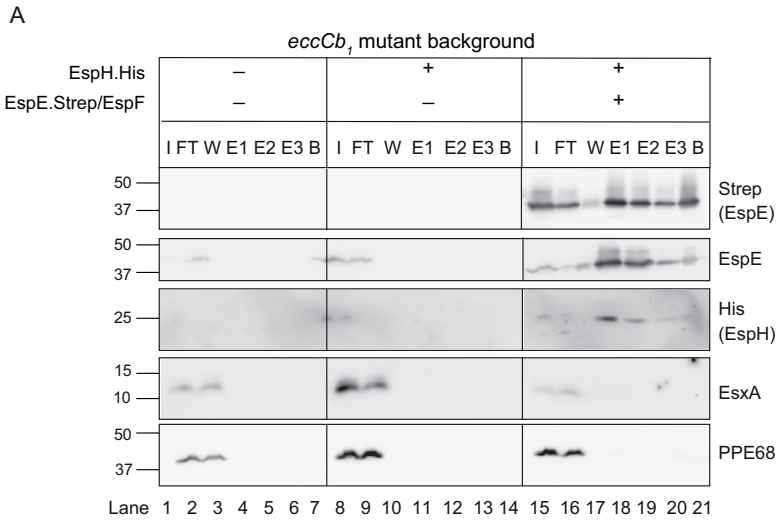


**Figure 5. EspH specifically interacts with EspE in *M. marinum*.**

[A] Immunoblots of pull-down assays using Strep-tactin agarose. EspE-Strep was purified from soluble lysates of the *eccCb*, mutant expressing only EspE-Strep/EspF or EspE-Strep/EspF together with EspH-His. A strain containing empty plasmids was included as negative control. Total input material (I), unbound proteins (FT), the final washing step (W), three fractions of eluted proteins (E1, E2, E3) and boiled beads fractions were separated by SDS-PAGE and further immunoblotted using antisera directed against the Strep- or His-tag. The elution fractions were loaded 10 times more compared to the other fractions. Endogenous EspE, PPE68 and EsxA substrates were detected using anti-EspE, anti-PPE68 and anti-EsxA, respectively. [B] Immunoblots of pull-down assays using Ni-NTA beads. EspH-His proteins were purified from soluble lysates of the *eccCb*, strain carrying a plasmid expressing EspH-His or the corresponding empty plasmid. Total input material (I), unbound proteins (FT), the last washing step (W), proteins eluted with 50 mM (E1), 100 mM (E2), and 200 mM (E3) imidazole and boiled bead fraction were separated by SDS-PAGE and probed with His-specific antiserum. The elution fractions were loaded 10 times more compared to the other fractions. Endogenous EspE, PPE68 and EsxA proteins were detected using anti-EspE, anti-PPE68 and anti-EsxA, respectively.

*espH* and *eccA*, differently affected the secretion of EsxA, we examined to what extent these mutant strains were able to disrupt erythrocytes. While we confirmed that our WT strain was able to show hemolysis (Figure 6A), both the *eccCb*<sub>1</sub> and  $\Delta$ *espG*<sub>1</sub> mutant strain lost this ability, in line with the absence of all ESX-1 substrates (Figure 6A). Interestingly, the  $\Delta$ *espH* and  $\Delta$ *eccA*<sub>1</sub> strains were also non-hemolytic, although these strains were still able to secrete EsxA to significant levels (Figure 6A). This finding is in line with a recent publications, which indicated that the ESX-1 mediated cell-membrane lysis is not directly linked to the pore-forming activity of EsxA (Conrad et al., 2017). The defects in hemolysis by the knockout strains were restored when the complemented plasmids were introduced into these mutant strains (Figure 6B). As in the  $\Delta$ *espH* and  $\Delta$ *eccA*<sub>1</sub> mutants mainly the secretion of different Esp proteins are specifically affected, our findings indicate that not a single ESX-1 substrate, such as EsxA, but a combination of different Esp proteins, are responsible for the hemolytic phenotype.

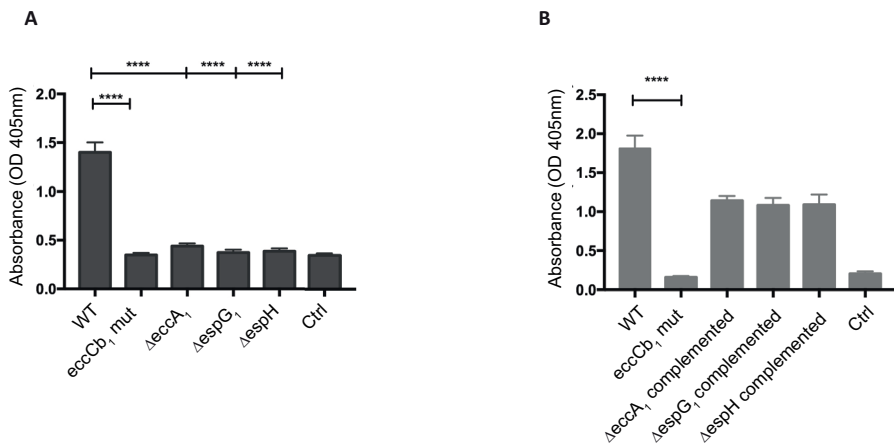


**Figure 6. All ESX-1 mutant strains have lost hemolytic activity.**

Contact-dependent hemolysis of red blood cells (RBCs) by various *M. marinum* strains grown in the presence of Tween-80. Hemolysis was quantified by determining the OD<sub>405</sub> absorption of the released hemoglobin. The data shown here is generated from two independent experiments, each time in triplicates.

### The role of individual ESX-1 accessory proteins in infection of phagocytic cells

To further characterize the function of the different ESX-1 substrate subsets, we used different phagocytic cells to study the ability of the mutant strains to survive and replicate within these cells. Phagocytic cells from mice (RAW macrophage cell line) and the protozoa *Acanthamoeba castellanii* were infected with green fluorescent protein (GFP)-expressing mycobacteria and infection levels were quantified by flow cytometry at different time points. With this method, we confirmed the previously shown ability of WT *M. marinum* to survive and replicate within these different phagocytic cells by

showing a 2-fold increase in percentage of infected cells between 3 and 24 hpi (Figure 7; (Weerdenburg et al., 2015)). As shown before, the ESX-1 secretion deficient *eccCb<sub>1</sub>* mutant was strongly attenuated, showing a 2-fold reduction in the number of infected cells after 24 h in both *A. castellanii* and RAW cells (Figure 7; (Weerdenburg et al., 2015)). As expected, based on the proteome profiles, the  $\Delta espG_1$  strain showed an attenuated phenotype similar to the *eccCb<sub>1</sub>* mutant in both infection models. For the  $\Delta espH$  mutant, the proportion of infected *A. castellanii* cells did not change over time (Figure 7B), while in RAW macrophages a slight reduction of infected cells at 24 hpi (Figure 7C,  $p = ns$ ) and a fold change between 3 and 24 hpi was observed (Figure 7D). Interestingly, infection with the  $\Delta eccA_1$  mutant resulted in an increase of infected cells over time, for both *A. castellanii* and RAW cells, and was therefore less attenuated as compared to the other mutants (Figure 7B, D). Although this strain was able to infect *A. castellanii* to the same extent as the WT strain, infection with this mutant was not as successful as WT infection in RAW macrophages (Figure 7A,  $ns$ ; Figure 7C,  $p < 0.001$ ).

Taken together, our data show the importance of *espG<sub>1</sub>* in achieving successful infection of phagocytic cells, while the loss of *eccA<sub>1</sub>* only marginally affects the ability of *M. marinum* to survive and replicate in a phagocytic host cell. These findings are in line with the proteomic analysis, *i.e.* the *espG<sub>1</sub>* mutation has a strong effect on secretion of all ESX-1 substrates, while deleting *eccA<sub>1</sub>* only results in a mild secretion defect. EspH, which mainly seems to influence EspE and EspF secretion, is also important for infecting phagocytes, but to a lesser extent than EspG<sub>1</sub>.

### ***In vivo* virulence phenotype of *eccA<sub>1</sub>* and *espG<sub>1</sub>* mutant strains is similar to their *in vitro* phenotype**

To study whether the individual ESX-1 proteins play a role during infection *in vivo*, we used the zebrafish larva-*M. marinum* infection model. Larvae were systemically infected with the fluorescently labeled knockout strains and infection was analyzed 4-days post infection (dpi) by fluorescence microscopy to examine overall infection rate. In addition, L-plastin staining was performed to visualize phagocytic cells in order to study the formation of early granulomas by confocal microscopy.

Infection of zebrafish larvae with the  $\Delta espG_1$  and  $\Delta eccA_1$  mutant strains resulted in infection levels as expected from the previous experiments, *i.e.* the  $\Delta espG_1$  showed a similar level of attenuation as the *eccCb<sub>1</sub>* mutant, while the  $\Delta eccA_1$  mutant infections were similar to wildtype infection (Figure 8A, D, H for  $\Delta eccA_1$ ; Figure 8B, F, J for  $\Delta espG_1$ ). Higher magnification of individual infection loci in  $\Delta eccA_1$  infected larvae revealed recruitment of phagocytic cells and formation of early granulomas comparable to infection with WT (Figure 8E for WT,  $n=12$  larvae; Figure 8I for  $\Delta eccA_1$ ,  $n=8$  larvae). In contrast, confocal imaging of  $\Delta espG_1$  infected fish showed a predominance of single infected macrophages and formation of very small clusters of these infected macrophages similar to infection

with the *eccCb<sub>1</sub>* mutant (Figure 8G for *eccCb<sub>1</sub>* mutant, n=10 larvae; Figure 8K for  $\Delta espG_1$ , n=7 larvae).

Together, this shows that *espG<sub>1</sub>*, but not *eccA<sub>1</sub>*, plays a major role in early stages of infection *in vivo*. Moreover, since these strains show a comparable behavior during *in vitro* and *in vivo* infections, this indicates functional similarities for these genes in protozoa, mouse macrophages and zebrafish larvae.

### *Acanthamoeba castellanii*

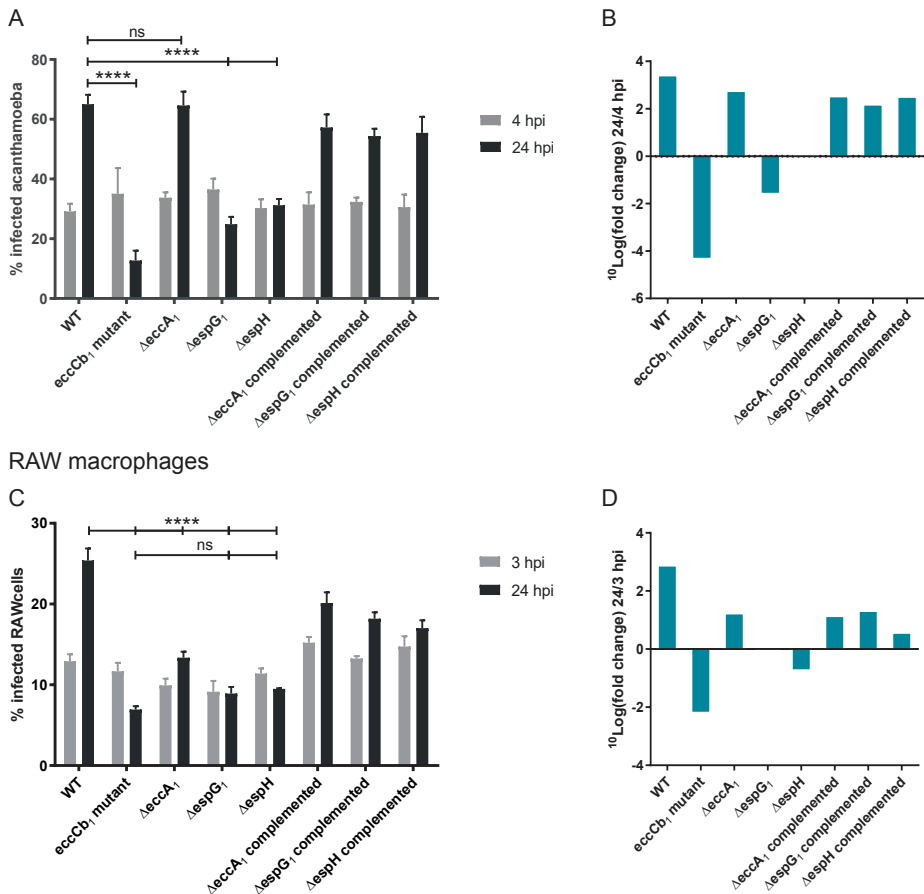


**Figure 7. Intracellular growth of  $\Delta eccA_1$ ,  $\Delta espG_1$  and  $\Delta espH$  in different hosts**

[A] Flow cytometry experiment showing percentage of infected *A. castellanii* at 3 hours post infection (hpi) versus 24 hpi, graph shows pooled data from two independent experiments. [B] Graph shows fold change in percentage infected *A. castellanii* presented in A. [C] Similar flow cytometry experiment with infected RAW macrophages when comparing percentage infected cells at 3hpi and 24 hpi, graph shows representative data of 1 out of 3 biological replicates. [D] Graph shows fold change in percentage infected RAW macrophages presented in C. \*\*\*\* =  $p < 0.0001$ , ns = non-significant

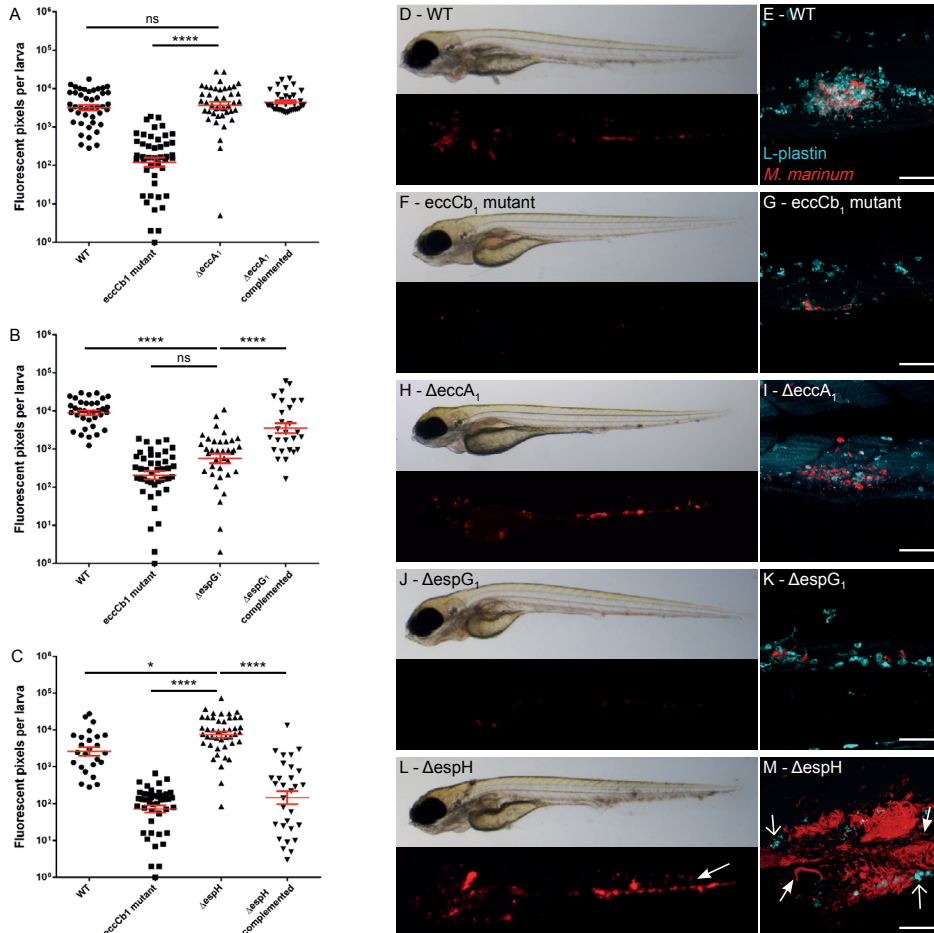


**Figure 8. In vivo effect of  $\Delta eccA_1$ ,  $\Delta espG_1$  and  $\Delta espH$  in zebrafish larvae**

Graphs A-C show relative levels of infection as determined by automated pixel count software for infection of zebrafish larvae. The larvae were infected with ~75-150 CFU red fluorescent *M. marinum* mutant strains and analyzed at 4 dpi. Graphs show combined data of three independent biological replicates per mutant strain, each dot represents one larva. Bars represent mean and standard error of the mean. [A] Systemic infection of zebrafish larvae with *M. marinum*  $\Delta eccA_1$ , [B] *M. marinum*  $\Delta espG_1$ , and [C] *M. marinum*  $\Delta espH$ , \* = <0.05, \*\*\*\* <0.001.

Representative bright field and corresponding fluorescent images are depicted in: [D] WT infection, [F] *eccCb1* mutant infection, [H] *M. marinum*  $\Delta eccA_1$ , [J] *M. marinum*  $\Delta espG_1$ , [L] *M. marinum*  $\Delta espH$ . Confocal imaging of a single cluster of infected L-plastin labeled phagocytic cells (cyan) in the tail of infected larvae confirmed the phenotype seen in fluorescent imaging: [E] WT infection, [G] *eccCb1* mutant infection, [I] *M. marinum*  $\Delta eccA_1$ , [K] *M. marinum*  $\Delta espG_1$ , [M] *M. marinum*  $\Delta espH$ , depicting a cording phenotype (closed arrows) and intense fluorescent spots suggestive for phagocytic cell debris (open arrows). Scale bar E, G, I, K, M = 50  $\mu$ m

### The absence of *espH* results in a hypervirulent phenotype in zebrafish larvae

In contrast to the  $\Delta espG_1$  and  $\Delta eccA_1$  strain, the behavior of  $\Delta espH$  in zebrafish larvae was completely different from its attenuated phenotype *in vitro*. Systemic infection

of zebrafish larvae resulted in an increased bacterial load compared to WT infection (Figure 8C;  $p < 0.05$ ). Large bacterial clusters and a phenotype known as cording were seen in fluorescence images (Figure 8L, arrow) and especially at higher magnification of individual clusters (Figure 8L, closed arrow,  $n = 15$  larvae). Cording in zebrafish has been associated with extracellular growth (Clay et al., 2008). In addition, very limited numbers of intact phagocytic cells and the presence of fluorescent spots suggestive for phagocytic cell debris were observed (Figure 8L, open arrow).

These observations raised the question whether this phenotype is still preceded by granuloma formation or if this mutant strain is preventing early granuloma formation by inducing rapidly host cell death. Therefore, larvae were systemically infected with either  $\Delta espH$  or WT *M. marinum* as control and monitored daily for 4 consecutive days (Figure 9). Mycobacteria were phagocytosed by L-plastin positive phagocytic cells at 1 dpi in both groups (Figure 9A, D). Subsequently, phagocytic cells were recruited and early granulomas started to form (Figure 9B, E). However, at 4 dpi, in larvae infected with the  $\Delta espH$  mutant strain a strong decrease in phagocytic cells and increase in bacterial growth was observed (Figure 9C, F). In the absence of phagocytic cells bacteria were

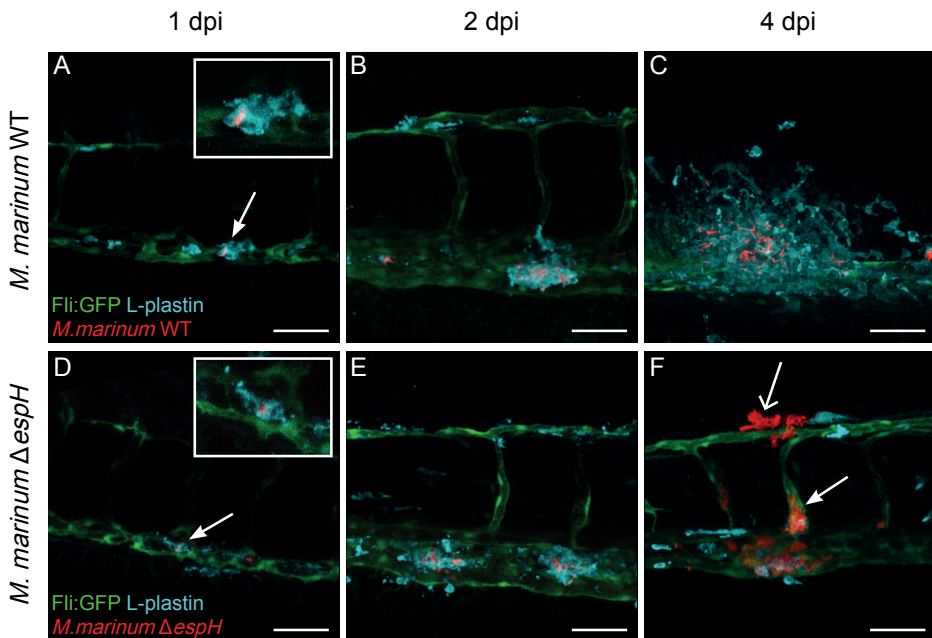


**Figure 9. *EspH*-mutant strain is hypervirulent in zebrafish larvae**

[A-C] Systemic *M. marinum* WT infection (red) of *Tg(fli:GFP)* larvae with green fluorescent blood vessels was followed over time, representative images are shown in A. 1 dpi, B. 2dpi, C. 4dpi. Larvae were stained with anti-L-plastin to label phagocytic cells (cyan). [D-F] Representative images of systemic infection with *M. marinum*  $\Delta espH$  over time in D. 1 dpi, E. 2dpi, F. 4dpi. Scale bar = 50  $\mu$ m

able to show cording in both blood vessels (Figure 9F, closed arrow) and tissue (Figure 9F, open arrow).

Taken together, the  $\Delta espH$  mutant seems to have a host specific or *in vivo* specific effect, illustrated by a hypervirulent phenotype seen in zebrafish larvae but not in cell infections *in vitro*. Therefore, our data indicates that EspH is not required for initial phagocytosis, recruitment of cells and primary establishment of early granulomas, but EspH, and therefore a subset of ESX-1 substrates, seems to be essential for the maintenance of a stable granuloma.

## DISCUSSION

A number of studies have shown that the mycobacterial ESX-1 system plays a pivotal role in mycobacterial pathogenesis (Brodin et al., 2006; Fortune et al., 2005; Hsu et al., 2003; Lewis et al., 2003). The system affects virulence through secretion of protein effectors with host-modulatory effects. A currently well-accepted model is that ESX-1 (and other T7SS) substrates are usually secreted as folded heterodimers, where one of the partners is carrying the general secretion signal of a helix-turn-helix followed by the motif YxxxD/E, which is required for recognition by the secretion system (Maria H. Daleke et al., 2012). In addition, the PE/PPE heterodimeric substrates are maintained in secretion-competent state by the dedicated molecular chaperone EspG. The substrates are then targeted to the secretion machinery, where the translocation of the substrates takes place with an involvement of the AAA+ ATPase EccA<sub>1</sub>. However, numerous questions remain about the mode of recognition of the different ESX-1 substrate subsets and the role of EspG<sub>1</sub> and EccA<sub>1</sub> in this process: does EspG indeed function as a specific chaperone of PE/PPE proteins and if so, do the other ESX-1 substrates depend on other chaperones to keep them in a secretion-competent state?

In this study, we show that EccA<sub>1</sub> is not strictly required for the secretion of ESX-1 substrates. The finding that EccA<sub>1</sub> is important for secretion is in line with previous reports (Gao et al., 2004; Joshi et al., 2012), but the finding that the role of EccA<sub>1</sub> is depending on the growth medium is entirely surprising. This difference could also explain the variable results described for the role of EccA<sub>1</sub> in EsxA secretion by *M. tuberculosis* (E. N. G. Houben et al., 2012). Of all ESX-1 substrates, EspE, EspF, EspJ and EspK secretion was mostly reduced in our *eccA<sub>1</sub>* mutant strain, while secretion of EspB, EsxA/EsxB and PE/PPE was hardly affected. Two possible explanations for the reduction of EspE/EspF secretion exist. The first possibility is that EccA<sub>1</sub> directly recognizes the affected Esp proteins and that this recognition is necessary for their secretion. This hypothesis is supported by the fact that EspC, the homologous protein of EspF, interacts with EccA<sub>1</sub> via the C terminal domain, which is required for secretion (DiGiuseppe Champion et al., 2009;

Fortune et al., 2005; Lou et al., 2017). In this scenario, the slight reduction in secretion of the other ESX-1 substrates could be due to the interdependent secretion of the different substrates. The second possible explanation involves EccA<sub>1</sub>'s suggested contribution to mycobacterial cell envelope synthesis, as a strain containing a transposon insertion in *eccA*<sub>1</sub> makes less mycolic acid as compared to strains expressing wild-type EccA<sub>1</sub> (Joshi et al., 2012). Therefore, it is tempting to speculate that the significant decrease in Esp secretion is a consequence of failure to properly associate with the altered cell envelope in the absence of EccA<sub>1</sub> function, rather than a secretion block in the ESX-1 system.

An interesting observation in our study is the discrepancy between the active secretion of EsxA in the  $\Delta eccA_1$  strain and at the same time loss of hemolytic activity. Although this observation has been described before, this was always linked to a reduced secretion of EsxA in these strains (Gao et al., 2004; Joshi et al., 2012). Recently, the importance of EsxA in lysing membranes was questioned, showing that lytic activity of purified EsxA only occurred at low pH conditions, while the hemolysis assay is carried out at neutral pH, and that ESX-1-mediated cell lysis occurs through a contact-dependent mechanism (Conrad et al., 2017). Our results support this alternative explanation: we find a strong correlation between ESX-1 functionality and hemolysis, but this correlation is not seen for EsxA secretion. We therefore propose that it is not the loss of secreted EsxA, but the loss of (multiple) surface-exposed Esp proteins that results in hemolytic deficiency.

Even though the  $\Delta eccA_1$  strain lost its ability to induce membrane lysis, virulence in isolated phagocytes and in zebrafish larvae was only mildly affected in our study. This is in contrast with different groups describing an attenuated phenotype in murine macrophages and zebrafish (Gao et al., 2004; Joshi et al., 2012). The latter observations were made after a longer incubation time, which might explain the discrepancy with our study. Distinct phenotypes of the *eccA*<sub>1</sub> mutant in different host cells have also been reported in a genome-wide transposon mutagenesis study (Weerdenburg et al., 2015). Here, transposon insertions in *M. marinum* E11 *eccA*<sub>1</sub> led to severe attenuation in mammalian phagocytic cells but these mutants were hypervirulent in protozoan cells (Weerdenburg et al., 2015). This suggests that *M. marinum* can employ host-specific virulence mechanisms to adapt to different intracellular environments and that EccA<sub>1</sub> might be essential for secretion and virulence under specific circumstances or in a subset of specific hosts. The hypothesis that EccA<sub>1</sub> only plays an important role in ESX-1 dependent secretion under specific conditions is supported by our observation that that the effect of the *eccA*<sub>1</sub> deletion on secretion is more significant when the bacteria were grown under nutrient-limited conditions.

The role of EspG as a specific chaperone for the recognition and secretion of cognate PE/PPE proteins has been well established in *M. marinum* (Maria H. Daleke et al., 2012; Phan et al., 2017). Our extracellular proteomic study not only confirms the loss of PE/PPE substrate secretion in the *M. marinum*  $\Delta espG_1$  strain, but it also shows that the absence

of EspG<sub>1</sub> also blocks the secretion of other ESX-1 dependent substrates, including EsxA/EsxB. Although this has been shown before in *M. marinum* (Phan et al., 2017), this phenotype is opposite to what was observed in an *M. tuberculosis* *espG*<sub>1</sub> knock-out strain. Possibly, there is redundancy in EspG functioning in *M. tuberculosis*. Moreover, two new putative substrates of the ESX-1 system were revealed by our proteome analysis, *i.e.* PE protein MMAR\_2894 and PPE protein MMAR\_5417, both of them carry the typical features of T7SS substrates such as a secretion signal YxxxD/E and a predicted helix-turn-helix structure. Possibly, these two proteins form a secreted heterodimer.

Structural studies showed that EspG proteins bind specifically to the extended helices of the PPE protein, which are absent in Esx proteins. Therefore, the strong effect of *espG*<sub>1</sub> deletion on Esx (and also Esp) protein secretion is likely indirect. A plausible explanation for the broad secretion defect is a mutual dependency in secretion among the ESX-1 substrates, a phenotype that has observed previously (Chen et al., 2012; Fortune et al., 2005; Phan et al., 2017). Recently, a study by Rosenberg et al. showed that simultaneous binding of multiple substrates to the ATPase domain of EccC is required for multimerization and activation of the secretion system (Rosenberg et al., 2015). One possible scenario is that PPE68 is unstable in the absence of the EspG<sub>1</sub> chaperone and thus not targeted to the secretion system, which in turn disables the activation of EccC, leading to the secretion block of the ESX-1 system.

Because of the severe secretion defect of all detectable ESX-1 substrates, the *M. marinum* *espG*<sub>1</sub> mutant becomes non-hemolytic and strongly attenuated in macrophage and amoeba, which is in good agreement with previous reports (Gao et al., 2004). Furthermore, we could confirm that the loss of *espG*<sub>1</sub> resulted in a strong attenuation in zebrafish, to the same extend as the *eccCb*<sub>1</sub> mutant. Similarly, reduced attenuation of an *M. tuberculosis* *espG*<sub>1</sub> knockout in mice was observed previously (Bottai et al., 2011)

EspH is specific for the ESX-1 secretion system, but is highly conserved among pathogenic mycobacterial species, including *M. tuberculosis* and *M. leprae*. The latter species has been streamlined into a minimal genome by a process of extensive genome decay, suggesting an important role for *espH* in mycobacterial pathogenesis. In our study, deletion of this gene specifically abolishes the expression and secretion of two specific ESX-1 substrates EspE and EspF. Furthermore, we could show that EspH specifically interacts with EspE in the cytosol. EspH shares high homology to EspD, another ESX-1-associated protein that was observed to act as a chaperone to stabilize intracellular EspA/EspC substrates (Chen et al., 2012). This indicates that EspH may function as a specific chaperone for its cognate substrates EspE/EspF. Using Phyre2 (Kelly et al., 2015) we discovered that EspH is predicted to share structural similarity to YbaB, an *E. coli* DNA-binding protein likely playing a regulatory role in the recovery of DNA replication (Lim et al., 2003). Recently, a structural study of *M. tuberculosis* EspL also revealed a high resemblance to YbaB (Tian et al., 2016), making it tempting to speculate that EspL may as well function

as a chaperone. It becomes clear that multiple chaperones, such as EspG<sub>1</sub>, EspD and EspH, are responsible for stabilizing their cognate substrates PE35/PPE68, EspC/EspA and EspF/EspE, respectively. Interestingly, other ESX-1 substrates were only marginally affected in the *espH* mutant, showing these substrates do not (strongly) depend on EspE/EspF for their secretion.

Deletion of *espH* also resulted in reduced secretion of EsxA/EsxB, which was not due to differences in mRNA levels. Interestingly, secretion of other substrates of the ESX-1 system, such as EspB, EspK and EspJ, did not seem to be affected by this mutation. A similar phenotype was observed previously in an *espA::tn* mutant of *M. tuberculosis* (Chen et al., 2013), where secretion of EsxA/EsxB but not EspB was aborted. This hints towards a possible regulation mechanism between the secretion of EsxA and Esp substrates but not among the Esp proteins themselves.

The *espH* mutant strain showed a loss of hemolytic activity and a reduction of intracellular growth in phagocytic host cells in our study. Strikingly, although EsxA/EsxB secretion was reduced, zebrafish larvae were heavily infected with this mutant strain with hypervirulence at later time points. More detailed analysis showed that initial phagocytosis and primary establishment of an early granuloma was not affected in this mutant, indicating that factors in addition to EsxA/EsxB might be involved in this process. A candidate might be EspB, whose secretion, was not affected in *espH* mutant strain, and was shown to be able to facilitate *M. tuberculosis* virulence *in vitro* and *in vivo* in an EsxA-independent way (Chen et al., 2013). Eventually, a stable cluster of immune cells could not be maintained in larvae infected with the *espH* mutant, with subsequent extracellular bacterial overgrowth and apparent phagocyte death. The discrepancy between *in vitro* and *in vivo* results indicate an essential role for a, yet unknown, host factor involved. It is tempting to speculate that EspE/EspF, the two proteins that are most severely affected by the *espH* deletion, interact with this host factor in order to induce the homeostatic balance between host and pathogen in developing granulomas.

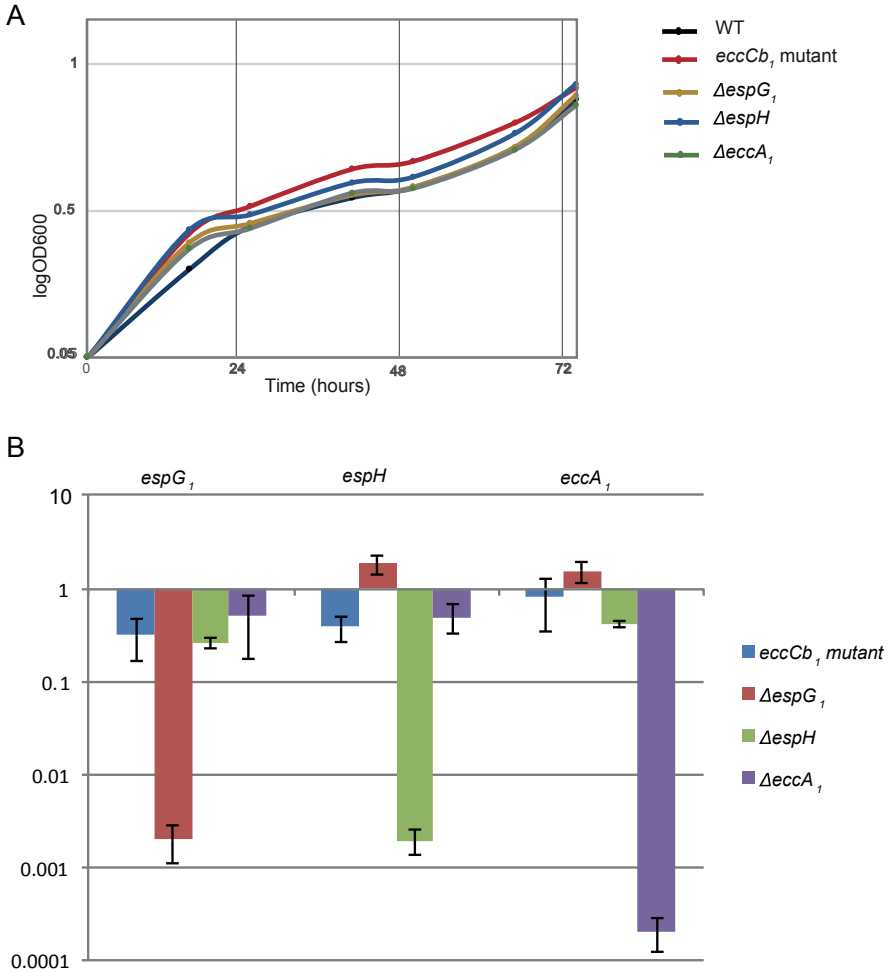
In summary, this study highlights the complexity of the ESX-1 secretion machinery. We unravel valuable information about the functions of the individual ESX-1 components EccA<sub>1</sub>, EspG<sub>1</sub> and EspH, all having their unique role in secretion of the different substrate classes. Furthermore, we show that EsxA secretion does not always correlate with different virulence read-outs, such as exhibiting hemolytic activity and mycobacterial growth *in vivo*, stressing the importance of the other ESX-1 substrates in mycobacterial virulence. We can conclude that ESX-1 has several different sets of substrates that are involved in different processes required for virulence.

## ACKNOWLEDGEMENTS

We would like to thank Joen Luirink for useful discussion. We thank Thang Pham and James Gallant for fruitful discussion and help with proteomic analysis. In addition, we thank James Gallant for development of custom-made fluorescent pixel counting software. We thank Gregory Koningstein, Theo Verboom and Wim Schouten for technical assistance, the imaging facility at AMC and VUmc for the use of their confocal microscope and Prof. P. Martin (Bristol University, UK) for the L-plastin antibody. We are grateful to Eric Brown (Genentech) for offering anti-EspE antibodies. This work was funded by a VIDI grant from the Netherlands Organization of Scientific Research (ENGH). The funders had no role in study design, data collection and analysis, decision to publish, or preparation of the manuscript.

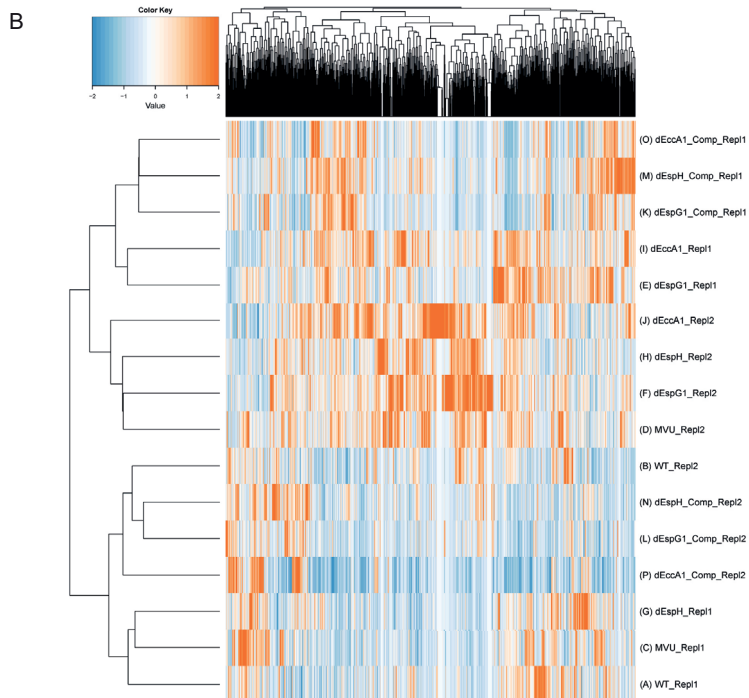
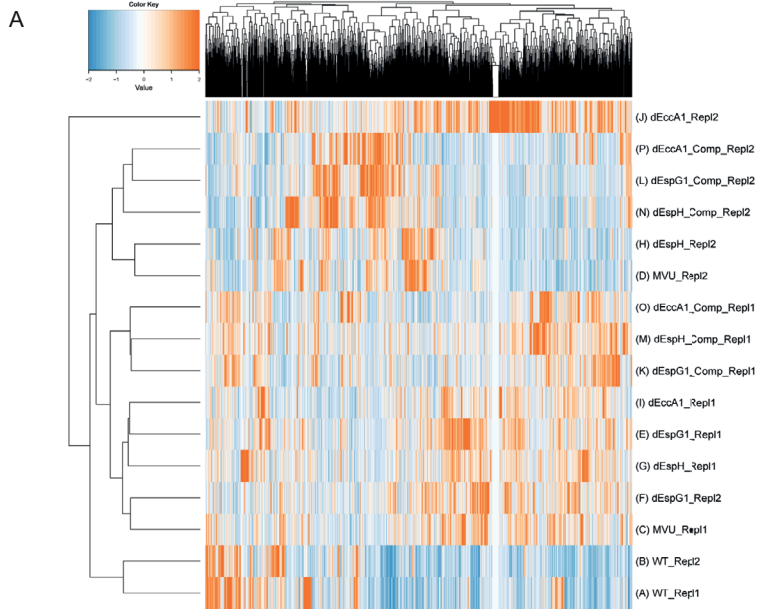
## SUPPLEMENTAL INFORMATION

Supplemental information includes supplemental experimental procedures and three figures.



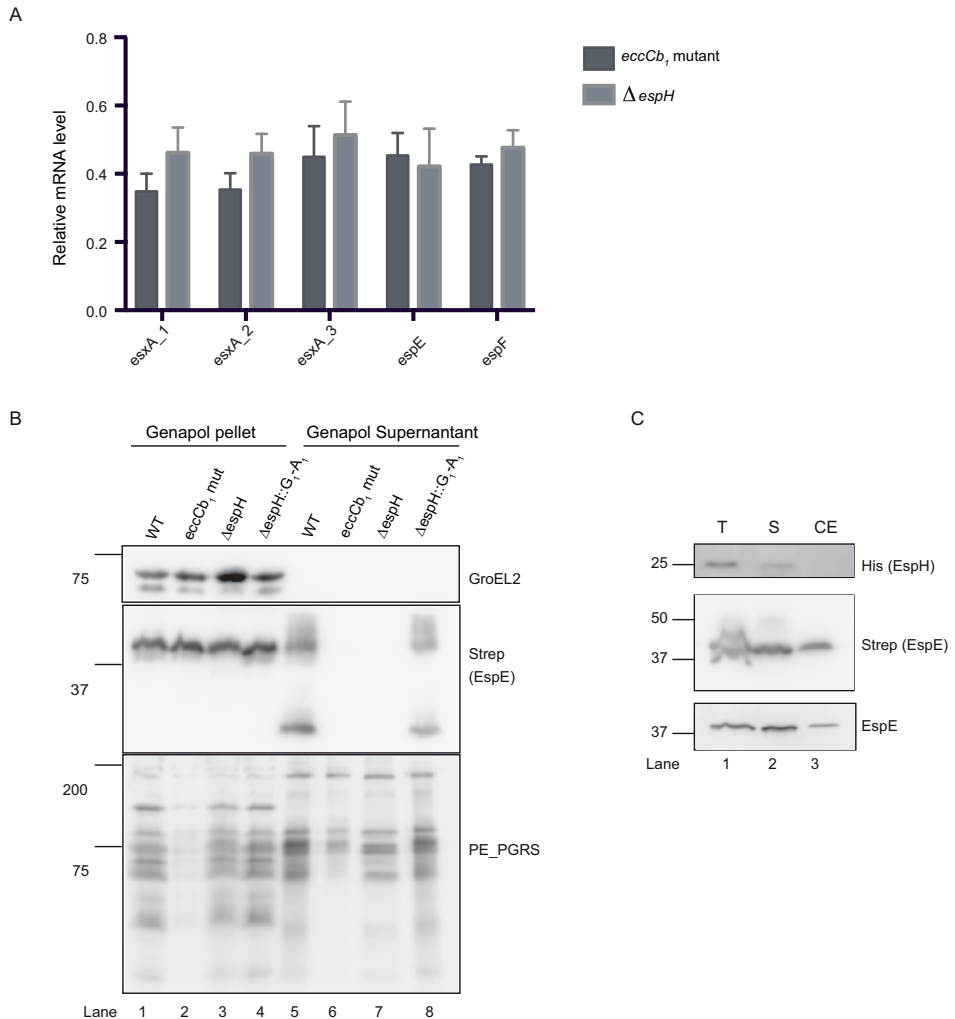
### Supplemental Figure S1

[A] The deletion of each ESX-1 component had no effect on the growth of the mutant strains. The WT *M. marinum* and studied ESX-1 knockout strains were grown in 7H9 supplemented with ADC and 0.05% Tween 80. The optical densities of the cultures were measured at a wavelength 600nm. Each color denotes each strain. [B] No polar effects caused by the deletion of each ESX-1 component to its adjacent genes. Total RNA was isolated from WT *M. marinum* M<sup>USA</sup> and the studied ESX-1 mutant strains. Specific primer sets were used to amplify *espG<sub>1</sub>*, *espH* and *eccA<sub>1</sub>* cDNA. Ct values were normalized for Ct values of the household gene *sigA* and compared to Ct values of the examined genes obtained from WT M<sup>USA</sup>.



**Supplemental Figure S2**

Heat map showing that the secretion defects in the  $\Delta espG$ ,  $\Delta espH$  and  $\Delta eccA$  mutants were restored by overexpressing the complementing plasmid pMV361::espF-eccA<sub>1</sub>. [A] Genapol-enriched fractions. [B] Supernatant fractions



### Supplemental Figure S3

[A] The deletion of *espH* had no effect on the transcription levels of *espE*, *espF* and *esxA*. Total RNA was isolated from WT *M. marinum* M<sup>USA</sup>, *eccCb<sub>1</sub>* mutant strain and the  $\Delta$ *espH* strain. Specific primer sets were used to amplified *espF* and *espE* cDNA. Also, three different sets of primers of *esxA*, including *esxA\_1*, *esxA\_2* and *esxA\_3*, were used for *esxA* cDNA. Ct values were normalized for Ct values of the household gene *sigA* and compared to Ct values of the examined genes obtained from WT M<sup>USA</sup>. [B] The C-terminally Strep-tagged *EspE* was secreted in the WT M<sup>USA</sup> and the  $\Delta$ *espH* complemented strain. Immunoblots of whole cells treated with Genapol (Genapol pellet) and 2-fold excess of Genapol supernatant from *M. marinum* WT strain M<sup>USA</sup>, the *eccCb<sub>1</sub>* mutant, the  $\Delta$ *espH* mutant and the  $\Delta$ *espH* complemented with the pMV361::*espG<sub>1</sub>-eccA<sub>1</sub>*, in which *espH* was C-terminally labeled with a 6xHis tag, all expressing *EspE*-Strep/*EspF*, were probed with antibodies against Strep, PE\_PGRS and the lysis control GroEL2. [C] *EspE* and *EspH* are soluble in the *M. marinum* *eccCb<sub>1</sub>* mutant. Immunoblot analysis of total (T), soluble (S), and cell envelope (CE) fractions of the *eccCb<sub>1</sub>* mut expressing *EspH*-His and *EspE*-Strep/*EspF*. *EspH* was detected using mAb directed against the His6 epitope, and *EspE* was checked using antibodies against both Strep and *EspE*.

**Supplemental Table S1. Strains used in this study**

Strains	Characteristics	References
MUSA	WT strain of <i>M. marinum</i>	
eccCb <sub>1</sub> mut (MVU)	<i>M. marinum</i> MUSA background strain containing the frame-shift mutation in eccCb <sub>1</sub>	Abdallah et al., 2009
ΔespG <sub>1</sub>	Complete deletion of espG <sub>1</sub> in the genome of <i>M. marinum</i> MUSA background strain	Phan et al., 2017
ΔespH	Complete deletion of espH in the genome of <i>M. marinum</i> MUSA background strain	this study
ΔeccA <sub>1</sub>	Complete deletion of eccA <sub>1</sub> in the genome of <i>M. marinum</i> MUSA background strain	this study

**Supplemental Table S2. Plasmids used in this study**

Plasmids	Characteristics	References
pMV::espF/espG <sub>1</sub> /espH/eccA <sub>1</sub>	hsp60 promoter, pMV361 backbone plasmid containing a region of espF/espG <sub>1</sub> /espH/eccA <sub>1</sub>	Current study
pMV::espG <sub>1</sub> /espH/eccA <sub>1</sub>	hsp60 promoter, pMV361 backbone plasmid containing a region of espG <sub>1</sub> /espH/eccA <sub>1</sub>	Phan et al., 2017
pSMT3::espE-Strep/espF	hsp60 promoter, pSMT3 backbone plasmid containing espE/espF in which espE is C-terminally tagged with Strep	Current study
pSMT3::meoS 3.1	hsp60 promoter, pSMT3 backbone containing mEoS3.1	Van Leeuwen et al, submitted, Meijer et al., 2008; Zhang et al., 2012
pMV361 empty	hsp60 promoter, pMV361 empty plasmid	

**Supplemental Table S3. Primers used in this study**

Purposes	Primer name	Sequence
ΔespH generation	espH KO LF	TTTTTTTTCACAAAGTGGCCAAACCCATAGCGAGTAG
	espH KO LR	TTTTTTTTCACCTTCGTGTGTGGCGTCCCTTTCTGAAC
	espH KO RF	TTTTTTTTCACAGAGTGGCGGCCGAAGCCGAGGTATT
	espH KO RR	TTTTTTTTCACCTTGTGCTAGTCCGGCGAGCATGTTG
ΔeccA <sub>1</sub> generation	eccA <sub>1</sub> KO LF	TTTTTTTTCACAAAGTGACATCCCGAAGAGGATCTG
	eccA <sub>1</sub> KO LR	TTTTTTTTCACCTTCGTGGTATCACCGTTCGTTGTAAC
	eccA <sub>1</sub> KO RF	TTTTTTTTCACAGAGTGGGAAACCAACGAGGGTCTAC
	eccA <sub>1</sub> KO RR	TTTTTTTTCACCTTGTGGCTCCCATTCCCAACACAAG
espG <sub>1</sub> qPCR	espG <sub>1</sub> qPCR FW	AACTGTACGGCAGCTTCCTC
	espG <sub>1</sub> qPCR RV	ATTAAGTCAACCTCGGGCGG
espH qPCR	espH qPCR FW	GATGCACTTCACGGGCTGAC
	espH qPCR RV	CATGTTTCGAGCCTTGTCTGG
eccA <sub>1</sub> qPCR	eccA <sub>1</sub> qPCR FW	TGGCCGAAGCCCAAGAAGAA
	eccA <sub>1</sub> qPCR RV	CTGACTGGCCCTCGTACTCG
espF qPCR	espF qPCR FW	GCGGCCGAGATCAGATTGTT
	espF qPCR RV	ACCCACGGCTCATTACCT
espE qPCR	espE qPCR FW	AGGAATCGCCGACAAGATGG
	espE qPCR RV	ATCAGGTTGCCGGTCAGATA
esxB qPCR	esxB qPCR FW	ATCTCCGGTGACCTGAAGAC
	esxB qPCR RV	TTCGGCCTTCTGCTTGTGG
esxA qPCR	esxA qPCR FW	GGCAGCATCCAGCGCAATTC
	esxA qPCR RV	AGCTTGTGCAGCGACTGCTT
sigA qPCR	sigA_FW	TCGAGGTGATCAACAAGCTG
	sigA_RV	ATTTCTTTGGCCAGCTCCTC
pMV::espF/espG <sub>1</sub> / espH/eccA <sub>1</sub>	F_Pacl_espF	TCTCTTAATTAACGGCTCACTGGCCTACCAAA
	R_EccA1_HindIII	GGGGGGAAGCTTTCACTCTCTCATATTGAGGTGTG
pMV::espG <sub>1</sub> / espH.His/eccA <sub>1</sub>	Fw_Pacl_EspG1	GGGGGGTTAATTAATGACCGGTCCGCTCG
	Rv_EspH_His	TCAATGGTGGTGGTATGATGCCGTTCTGTTGAACGAGAGGTG
	Rv_EccA1_HindIII	GGGGGGAAGCTTTCACTCTCTCATATTGAGGTGTG
pSMT3::espE.Strep/ espF	Fw_His tag_EccA1	CATCATCACCACCACCATTGATACGACTGATCGCCTGGCC
	EspF Fw	GAGGAAAGGTCTACCCCATGTATCCGTATGATGTTCTGATTATGCT ACAGGACTACTGAACGTCGTG
	EspF_Rv	AGCATAATCAGGAACATCATA CGGATACATGGGGGTAGACCTTTCCTC
	espE_strep Rv	CTACTTCTCGAACTGCGGATGCGACCAGAGGAGGGTCCCTCG
	Strep_espF Fw	CGAGGGGACCCCTCTCTGGTCCGATCCGCAGTTCGAGAAGTAGTCC- GGGCAACCG
	Fw EspE NheI	CCCCCGTAGCATGGTGCCAAAGGGAAG

### Supplemental Table S4.

The averages (replicates of two) of normalized spectral counts and the fold changes of the ESX-1 substrates in different ESX-1 mutants compared to the WT strain are presented. [A] in Genapol-enriched fraction, [B] in the supernatant fraction

A:

Gene.names	Average count WT	Average count eccCb1 mut	Fold change	p-value	Average count ΔespG <sub>1</sub>	Fold change	p-value	Average count ΔespH	Fold change	p-value	Average count ΔeccA1	Fold change	p-value
2894 (PE)	40,9	1,5	-28,01	0,00014	0,4	-94,26	0,00021	33,6	-1,22	0,35057	20,1	-2,03	0,01746
5417 (PPE)	17,8	0,4	-41,94	0,01629	0,0	-10000,00	0,00454	29,6	1,66	0,17836	5,2	-3,43	0,07106
EspA	6,3	0,0	-10000,00	0,00279	7,0	1,12	0,40373	37,6	5,99	0,10811	29,0	4,63	0,00090
EspB	431,2	15,4	-28,07	0,00049	27,5	-15,66	0,00074	305,5	-1,41	0,10982	142,3	-3,03	0,00573
EspC	14,8	0,0	-10000,00	0,00168	9,2	-1,61	0,17427	29,0	1,96	0,07240	30,2	2,04	0,01250
EspE	325,5	18,6	-17,53	0,00000	15,3	-21,25	0,00005	2,5	-132,80	0,00000	41,2	-7,91	0,00001
EspF	547,2	31,9	-17,15	0,00004	16,6	-32,91	0,00009	2,7	-204,19	0,00004	54,7	-10,01	0,00004
EspJ	27,5	0,4	-64,74	0,00045	1,8	-15,71	0,00057	10,0	-2,76	0,00480	0,4	-62,45	0,00049
EspK	278,2	2,9	-95,18	0,00000	14,0	-19,84	0,00036	157,6	-1,76	0,00026	28,5	-9,76	0,00000
EsxA	252,0	23,9	-10,56	0,00089	38,1	-6,62	0,00415	181,6	-1,39	0,23554	184,4	-1,37	0,12907
EsxA_1	3,9	0,0	-10000,00	0,00609	0,0	-10000,00	0,00526	1,6	-2,46	0,29043	3,5	-1,12	0,83658
EsxB_1	222,4	36,2	-6,15	0,00004	56,0	-3,97	0,00477	96,1	-2,31	0,00069	91,7	-2,42	0,00086
PPE68	159,6	1,6	-96,84	0,00008	1,3	-122,53	0,00026	104,1	-1,53	0,04494	38,5	-4,14	0,00090

B:

Gene.names	Average count WT	Average count eccB1 mut	Fold change	p-value	Average count ΔespG <sub>1</sub>	Fold change	p-value	Average count ΔespH	Fold change	p-value	Average count ΔeccA1	Fold change	p-value
2894 (PE)	9,1	0	-10000	0,00085	0	-10000	0,00076	5,0	-1,83	0,13282	3,9	-2,34	0,03506
5417 (PPE)	0,0	0	1	1	0	1	0,99999	0,4	10000	0,26117	0,8	10000	0,14695
EspA	2,3	0	-10000	0,02306	0,4	-5,88	0,10057	5,1	2,26	0,16447	9,0	3,95	0,00852
EspB	221,4	16,5	-13,45	5,46E-06	12,2	-18,17	2,53E-05	176,5	-1,25	0,01599	63,0	-3,51	1,52E-05
EspC	2,8	0	-10000	0,00971	1,2	-2,44	0,29183	2,7	-1,04	0,93162	3,6	1,27	0,69451
EspE	17,0	2,9	-5,90	0,12504	1,3	-13,08	0,06778	0	-10000	0,00885	1,9	-8,74	0,08469
EspF	14,2	1,3	-10,61	0,00287	2,5	-5,77	0,00346	0	-10000	0,00047	1,9	-7,31	0,00117
EspJ	25,6	1,7	-14,71	0,00036	1,8	-14,05	0,00023	20,1	-1,27	0,24376	3,3	-7,84	0,00047
EspK	106,7	6,1	-17,35	2,35E-05	6,5	-16,45	2,28E-05	43,7	-2,44	0,00032	5,1	-20,86	1,41E-05
EsxA	334,9	37,9	-8,83	3,56E-06	16,3	-20,49	4,12E-06	55,5	-6,03	1,95E-05	61,8	-5,42	3,92E-06
EsxB_1	299,4	28,9	-10,35	3,32E-05	20,9	-14,32	2,43E-05	98,4	-3,04	0,00102	107,9	-2,78	0,00020
MalK	2,3	6,3	2,80	0,05790	7,4	3,27	0,03552	6,1	2,68	0,08292	5,4	2,38	0,09577
PPE68	10,2	0,4	-22,89	0,00433	0	-10000	0,00186	6,3	-1,61	0,33986	3,0	-3,40	0,02439
SecA2	0,6	1,5	2,69	0,34260	3,2	5,67	0,12375	1,7	2,99	0,40277	1,7	2,93	0,32223

## REFERENCES

- Abdallah, A.M., Gey van Pittius, N.C., DiGiuseppe, P.A., Cox, J., Luirink, J., Vandenbroucke-Grauls, C.M.J.E., Appelmelk, B.J., Bitter, W., 2007. Type VII secretion--mycobacteria show the way. *Nat. Rev. Microbiol.* 5, 883–91. doi:10.1038/nrmicro1773
- Abdallah, A.M., Verboom, T., Hannes, F., Safi, M., Strong, M., Eisenberg, D., Musters, R.J.P., Vandenbroucke-Grauls, C.M.J.E., Appelmelk, B.J., Luirink, J., Bitter, W., 2006. A specific secretion system mediates PPE41 transport in pathogenic mycobacteria. *Mol. Microbiol.* 62, 667–679. doi:10.1111/j.1365-2958.2006.05409.x
- Abdallah, A.M., Verboom, T., Weerdenburg, E.M., Gey van Pittius, N.C., Mahasha, P.W., Jiménez, C., Parra, M., Cadieux, N., Brennan, M.J., Appelmelk, B.J., Bitter, W., 2009. PPE and PE\_PGRS proteins of *Mycobacterium marinum* are transported via the type VII secretion system ESX-5. *Mol. Microbiol.* 73, 329–340. doi:10.1111/j.1365-2958.2009.06783.x
- Allen, B.W., 1998. *Mycobacteria: General Culture Methodology and Safety Considerations.* Methods Mol. Biol. 101, 24. doi:10.1385/0-89603-471-2:15
- Andersen, P., Andersen, A., Sørensen, L., Nagai, S., 1995. Recall of long-lived immunity to *Mycobacterium tuberculosis* infection in mice. *J. Immunol.* 154, 3359–3372.
- Ates, L.S., Houben, E.N.G., Bitter, W., 2016. Type VII Secretion: A Highly Versatile Secretion System. *Microbiol. Spectr.* 4, 1–21. doi:10.1128/microbiolspec.VMBF-0011-2015.Correspondence
- Ates, L.S., Ummels, R., Commandeur, S., van der Weerd, R., Sparrius, M., Weerdenburg, E., Alber, M., Kalscheuer, R., Piersma, S.R., Abdallah, A.M., et al., 2015. Essential Role of the ESX-5 Secretion System in Outer Membrane Permeability of Pathogenic Mycobacteria. *PLoS Genet.* 11, 1–30. doi:10.1371/journal.pgen.1005190
- Bardarov, S., Kriakov, J., Carriere, C., Yu, S., Vaamonde, C., McAdam, R.A., Bloom, B.R., Hatfull, G.F., Jacobs, W.R., 1997. Conditionally replicating mycobacteriophages: a system for transposon delivery to *Mycobacterium tuberculosis*. *Proc. Natl. Acad. Sci. U. S. A.* 94, 10961–6. doi:10.1073/pnas.94.20.10961
- Benard, E.L., van der Sar, A.M., Ellett, F., Lieschke, G.J., Spaik, H.P., Meijer, A.H., 2012. Infection of zebrafish embryos with intracellular bacterial pathogens. *J. Vis. Exp.* 61, 1–9. doi:10.3791/3781
- Bottai, D., Majlessi, L., Simeone, R., Frigui, W., Laurent, C., Lenormand, P., Chen, J., Rosenkrands, I., Huerre, M., Leclerc, C., Cole, S.T., Brosch, R., 2011. ESAT-6 secretion-independent impact of ESX-1 genes *espF* and *espG* on virulence of *Mycobacterium tuberculosis*. *J. Infect. Dis.* 203, 1155–1164. doi:10.1093/infdis/jiq089
- Braunstein, M., Espinosa, B.J., Chan, J., Belisle, J.T., Jacobs, W.R., 2003. SecA2 functions in the secretion of superoxide dismutase A and in the virulence of *Mycobacterium tuberculosis*. *Mol. Microbiol.* 48, 453–464. doi:10.1046/j.1365-2958.2003.03438.x
- Brodin, P., Majlessi, L., Marsollier, L., de Jonge, M.I., Bottai, D., Demangel, C., Hinds, J., Neyrolles, O., Butcher, P.D., et al., 2006. Dissection of ESAT-6 System 1 of *Mycobacterium tuberculosis* and impact on immunogenicity and virulence. *Society* 74, 88–98. doi:10.1128/IAI.74.1.88
- Carlsson, F., Joshi, S.A., Rangell, L., Brown, E.J., 2009. Polar localization of virulence-related *Esx-1* secretion in mycobacteria. *PLoS Pathog.* 5. doi:10.1371/journal.ppat.1000285
- Champion, M.M., Williams, E.A., Pinapati, R.S., Champion, P.A.D., 2014. Correlation of phenotypic profiles using targeted proteomics identifies mycobacterial *esx-1* substrates. *J. Proteome Res.* 13, 5151–5164. doi:10.1021/pr500484w

- Chen, J.M., Boy-Röttger, S., Dhar, N., Sweeney, N., Buxton, R.S., Pojer, F., Rosenkrands, I., Cole, S.T., 2012. EspD is critical for the virulence-mediating ESX-1 secretion system in *Mycobacterium tuberculosis*. *J. Bacteriol.* 194, 884–893. doi:10.1128/JB.06417-11
- Chen, J.M., Zhang, M., Rybniker, J., Boy-Röttger, S., Dhar, N., Pojer, F., Cole, S.T., 2013. *Mycobacterium tuberculosis* EspB binds phospholipids and mediates EsxA-independent virulence. *Mol. Microbiol.* 89, 1154–1166. doi:10.1111/mmi.12336
- Chen, X., Cheng, H.F., Zhou, J., Chan, C.Y., Lau, K.F., Tsui, S.K.W., Au, S.W. ngor, 2017. Structural basis of the PE–PPE protein interaction in *Mycobacterium tuberculosis*. *J. Biol. Chem.* 292, 16880–16890. doi:10.1074/jbc.M117.802645
- Clay, H., Volkman, H.E., Ramakrishnan, L., 2008. Tumor Necrosis Factor Signaling Mediates Resistance to *Mycobacteria* by Inhibiting Bacterial Growth and Macrophage Death. *Immunity* 29, 283–294. doi:10.1016/j.immuni.2008.06.011
- Conrad, W.H., Osman, M.M., Shanahan, J.K., Chu, F., Takaki, K.K., 2017. *Mycobacterial* ESX-1 secretion system mediates host cell lysis through bacterium contact-dependent gross membrane disruptions. *Proc. Natl. Acad. Sci.* 114, 1371–1376. doi:10.1073/pnas.1620133114
- Daleke, M.H., Ummels, R., Bawono, P., Heringa, J., Vandenbroucke-Grauls, C.M.J.E., Luirink, J., Bitter, W., 2012. General secretion signal for the mycobacterial type VII secretion pathway. *Proc. Natl. Acad. Sci.* 109, 11342–11347. doi:10.1073/pnas.1119453109
- Daleke, M.H., Van Der Woude, A.D., Parret, A.H.A., Ummels, R., De Groot, A.M., Watson, D., Piersma, S.R., Jiménez, C.R., Luirink, J., Bitter, W., Houben, E.N.G., 2012. Specific chaperones for the type VII protein secretion pathway. *J. Biol. Chem.* 287, 31939–31947. doi:10.1074/jbc.M112.397596
- De Leon, J., Jiang, G., Ma, Y., Rubin, E., Fortune, S., Sun, J., 2012. *Mycobacterium tuberculosis* ESAT-6 exhibits a unique membrane-interacting activity that is not found in its ortholog from non-pathogenic *Mycobacterium smegmatis*. *J. Biol. Chem.* 287, 44184–44191. doi:10.1074/jbc.M112.420869
- DiGiuseppe, P.A., Champion, M.M., Manzanillo, P., Cox, J.S., 2009. ESX-1 secreted virulence factors are recognized by multiple cytosolic AAA ATPases in mycobacteria. *Mol. Microbiol.* 73, 950–962. doi:10.1111/j.1365-2958.2009.06821.x
- Ekiert, D.C., Cox, J.S., 2014. Structure of a PE–PPE–EspG complex from *Mycobacterium tuberculosis* reveals molecular specificity of ESX protein secretion. *Proc. Natl. Acad. Sci.* 111, 14758–14763. doi:10.1073/pnas.1409345111
- Fortune, S.M., Jaeger, A., Sarracino, D.A., Chase, M.R., Sasseti, C.M., Sherman, D.R., Bloom, B.R., Rubin, E.J., 2005. Mutually dependent secretion of proteins required for mycobacterial virulence. *Proc. Natl. Acad. Sci. U. S. A.* 102, 10676–81. doi:10.1073/pnas.0504922102
- Fraga, J., Maranha, A., Mendes, V., Pereira, P.J.B., Empadinhas, N., Macedo-Ribeiro, S., 2015. Structure of mycobacterial maltokinase, the missing link in the essential GlgE-pathway. *Sci. Rep.* 5, 8026. doi:10.1038/srep08026
- Gao, L.-Y., Guo, S., McLaughlin, B., Morisaki, H., Engel, J.N., Brown, E.J., 2004. A mycobacterial virulence gene cluster extending RD1 is required for cytolysis, bacterial spreading and ESAT-6 secretion. *Mol. Microbiol.* 53, 1677–1693. doi:10.1111/j.1365-2958.2004.04261.x
- Griffin, J.E., Gawronski, J.D., DeJesus, M.A., Ioerger, T.R., Akerley, B.J., Sasseti, C.M., 2011. High-resolution phenotypic profiling defines genes essential for mycobacterial growth and cholesterol catabolism. *PLoS Pathog.* 7, 1–9. doi:10.1371/journal.ppat.1002251
- Gröschel, M.I., Sayes, F., Simeone, R., Majlessi, L., Brosch, R., 2016. ESX secretion systems: mycobacterial evolution to counter host immunity. *Nat. Publ. Gr.* 14, 677–691. doi:10.1038/nrmicro.2016.131
- Harboe, M., Malin, A.S., Dockrell, H.S., Gotten, H., Ulvund, G., Holm, A., Jørgensen, M.C., Wiker, H.G., 1998. B-Cell Epitopes and Quantification of the ESAT-6 Protein of *Mycobacterium tuberculosis* B-Cell

- Epitopes and Quantification of the ESAT-6 Protein of *Mycobacterium tuberculosis*. *Infect. Immun.* 66, 717–723.
- Houben, D., Demangel, C., van Ingen, J., Perez, J., Baldeón, L., Abdallah, A.M., Caleechurn, L., Bottai, D., van Zon, M., de Punder, K., et al., 2012. ESX-1-mediated translocation to the cytosol controls virulence of mycobacteria. *Cell. Microbiol.* 14, 1287–1298. doi:10.1111/j.1462-5822.2012.01799.x
- Houben, E.N.G., Bestebroer, J., Ummels, R., Wilson, L., Piersma, S.R., Jiménez, C.R., Ottenhoff, T.H.M., Lurink, J., Bitter, W., 2012. Composition of the type VII secretion system membrane complex. *Mol. Microbiol.* 86, 472–484. doi:10.1111/j.1365-2958.2012.08206.x
- Houben, E.N.G., Korotkov, K. V., Bitter, W., 2014. Take five - Type VII secretion systems of *Mycobacteria*. *Biochim. Biophys. Acta - Mol. Cell Res.* 1843, 1707–1716. doi:10.1016/j.bbamcr.2013.11.003
- Hsu, T., Hingley-Wilson, S.M., Chen, B., Chen, M., Dai, A.Z., Morin, P.M., Marks, C.B., Padiyar, J., Goulding, C., Gingery, M., et al., 2003. The primary mechanism of attenuation of bacillus Calmette-Guerin is a loss of secreted lytic function required for invasion of lung interstitial tissue. *Proc. Natl. Acad. Sci. U. S. A.* 100, 12420–12425. doi:10.1073/pnas.1635213100
- Joshi, S. a, Ball, D. a, Sun, M.G., Carlsson, F., Watkins, B.Y., Aggarwal, N., McCracken, J.M., Huynh, K.K., Brown, E.J., 2012. EccA1, a component of the *Mycobacterium marinum* ESX-1 protein virulence factor secretion pathway, regulates mycolic acid lipid synthesis. *Chem. Biol.* 19, 372–380. doi:10.1016/j.chembiol.2012.01.008
- Kelly, L.A., Mezulis, S., Yates, C., Wass, M., Sternberg, M., 2015. The Phyre2 web portal for protein modeling, prediction, and analysis. *Nat. Protoc.* 10, 845–858. doi:10.1038/nprot.2015-053
- Korotkova, N., Freire, D., Phan, T.H., Ummels, R., Creekmore, C.C., Evans, T.J., Wilmanns, M., Bitter, W., Parret, A.H.A., Houben, E.N.G., Korotkov, K. V., 2014. Structure of the *Mycobacterium tuberculosis* type VII secretion system chaperone EspG5 in complex with PE25-PPE41 dimer. *Mol. Microbiol.* 94, 1–20. doi:10.1158/2326-6066.CIR-13-0034.PD-L1
- Lewis, K.N., Liao, R., Guinn, K.M., Hickey, M.J., Smith, S., Behr, A., Sherman, D.R., 2003. Deletion of RD1 from *Mycobacterium tuberculosis* mimics Bacille Calmette-Guerin Attenuation. *J Infect Dis* 187, 117–123.
- Lim, K., Tempczyk, A., Parsons, J.F., Bonander, N., Toedt, J., Kelman, Z., Howard, A., Eisenstein, E., Herzberg, O., 2003. Crystal structure of YbaB from *Haemophilus influenzae* (HI0442), a protein of unknown function coexpressed with the recombinational DNA repair protein RecR. *Proteins Struct. Funct. Genet.* 50, 375–379. doi:10.1002/prot.10297
- Lou, Y., Rybniker, J., Sala, C., Cole, S.T., 2017. EspC forms a filamentous structure in the cell envelope of *Mycobacterium tuberculosis* and impacts ESX-1 secretion 103, 26–38. doi:10.1111/mmi.13575
- Mahairas, G.G., Sabo, P.J., Hickey, M.J., Singh, D.C., Stover, C.K., 1996. Molecular Analysis of Genetic Differences between *Mycobacterium bovis* BCG and Virulent *M. bovis* 178, 1274–1282.
- McLaughlin, B., Chon, J.S., MacGurn, J. a, Carlsson, F., Cheng, T.L., Cox, J.S., Brown, E.J., 2007. A mycobacterium ESX-1-secreted virulence factor with unique requirements for export. *PLoS Pathog.* 3, e105. doi:10.1371/journal.ppat.0030105
- Peng, X., Sun, J., 2017. Mechanism of ESAT-6 membrane interaction and its roles in pathogenesis of *Mycobacterium tuberculosis*. *Toxicon* 116, 29–34. doi:10.1007/s00210-015-1172-8.The
- Phan, T.H., Ummels, R., Bitter, W., Houben, E.N.G., 2017. Identification of a substrate domain that determines system specificity in mycobacterial type VII secretion systems. *Sci. Rep.* 7, 42704. doi:10.1038/srep42704
- Pym, A.S., Brodin, P., Brosch, R., Huerre, M., Cole, S.T., 2002. Loss of RD1 contributed to the attenuation of the live tuberculosis vaccines *Mycobacterium bovis* BCG and *Mycobacterium microti* 46, 709–717.

- Ramakrishnan, L., 2012. Revisiting the role of the granuloma in tuberculosis. *Nat. Rev. Immunol.* 12, 352–66. doi:10.1038/nri3211
- Refai, A., Haoues, M., Othman, H., Barbouche, M.R., Moua, P., Bondon, A., Mouret, L., Srairi-Abid, N., Essafi, M., 2015. Two distinct conformational states of *Mycobacterium tuberculosis* virulent factor early secreted antigenic target 6 kDa are behind the discrepancy around its biological functions. *FEBS J.* 282, 4114–4129. doi:10.1111/febs.13408
- Renshaw, P.S., Lightbody, K.L., Veverka, V., Muskett, F.W., Kelly, G., Frenkiel, T.A., Gordon, S. V., Hewinson, R.G., Burke, B., et al., 2005. Structure and function of the complex formed by the tuberculosis virulence factors CFP-10 and ESAT-6. *EMBO J.* 24, 2491–2498. doi:10.1038/sj.emboj.7600732
- Rosenberg, O.S., Dovala, D., Li, X., Connolly, L., Bendebury, A., Finer-Moore, J., Holton, J., Cheng, Y., Stroud, R.M., Cox, J.S., 2015. Substrates control multimerization and activation of the multi-domain ATPase motor of type VII secretion. *Cell* 161, 501–512. doi:10.1016/j.cell.2015.03.040
- Sani, M., Houben, E.N.G., Geurtsen, J., Pierson, J., De Punder, K., Van Zon, M., Wever, B., Piersma, S.R., Jiménez, C.R., Daffé, M., et al., 2010. Direct visualization by Cryo-EM of the mycobacterial capsular layer: A labile structure containing ESX-1-secreted proteins. *PLoS Pathog.* 6. doi:10.1371/journal.ppat.1000794
- Simeone, R., Bobard, A., Lippmann, J., Bitter, W., Majlessi, L., Brosch, R., Enninga, J., 2012. Phagosomal rupture by *Mycobacterium tuberculosis* results in toxicity and host cell death. *PLoS Pathog.* 8, e1002507. doi:10.1371/journal.ppat.1002507
- Smith, J., Manoranjan, J., Pan, M., Bohsali, A., Xu, J., Liu, J., McDonald, K.L., Szyk, A., LaRonde-LeBlanc, N., Gao, L.Y., 2008. Evidence for pore formation in host cell membranes by ESX-1-secreted ESAT-6 and its role in *Mycobacterium marinum* escape from the vacuole. *Infect. Immun.* 76, 5478–5487. doi:10.1128/IAI.00614-08
- Solomonson, M., Setiাপutra, D., Makepeace, K.A.T., Lameignere, E., Petrotchenko, E. V., Conrady, D.G., Bergeron, J.R., Vuckovic, M., Dimaio, F., Borchers, C.H., et al., 2015. Structure of EspB from the ESX-1 type VII secretion system and insights into its export mechanism. *Structure* 23, 571–583. doi:10.1016/j.str.2015.01.002
- Stoop, E.J.M., Schipper, T., Rosendahl Huber, S.K., Nezhinsky, A.E., Verbeek, F.J., Gurcha, S.S., Besra, G.S., Vandenbroucke-Grauls, C.M.J.E., Bitter, W., van der Sar, A.M., 2011. Zebrafish embryo screen for mycobacterial genes involved in the initiation of granuloma formation reveals a newly identified ESX-1 component. *Dis. Model. Mech.* 4, 526–536. doi:10.1242/dmm.006676
- Strong, M., Sawaya, M.R., Wang, S., Phillips, M., Cascio, D., Eisenberg, D., 2006. Toward the structural genomics of complexes: crystal structure of a PE/PPE protein complex from *Mycobacterium tuberculosis*. *Proc. Natl. Acad. Sci. U. S. A.* 103, 8060–8065. doi:10.1073/pnas.0602606103
- Tian, S., Chen, H., Sun, T., Wang, H., Zhang, X., Liu, Y., Xia, J., Guo, C., Lin, D., 2016. Expression, purification and characterization of Esx-1 secretion-associated protein EspL from *Mycobacterium tuberculosis*. *Protein Expr. Purif.* 128, 42–51. doi:10.1016/j.pep.2016.08.001
- van der Wel, N., Hava, D., Houben, D., Fluitsma, D., van Zon, M., Pierson, J., Brenner, M., Peters, P.J., 2007. *M. tuberculosis* and *M. leprae* translocate from the phagolysosome to the cytosol in myeloid cells. *Cell* 129, 1287–1298. doi:10.1016/j.cell.2007.05.059
- van der Woude, A.D., Stoop, E.J.M., Stiess, M., Wang, S., Ummels, R., van Stempvoort, G., Piersma, S.R., Cascioferro, A., Jiménez, C.R., Houben, E.N.G., et al., 2013. Analysis of SecA2-dependent substrates in *Mycobacterium marinum* identifies protein kinase G (PknG) as a virulence effector. *Cell. Microbiol.* 16, 280–295. doi:10.1111/cmi.12221

- Van Winden, V.J.C., Ummels, R., Piersma, S.R., Jiménez, C.R., Korotkov, K. V., Bitter, W., Houben, E.N.G., 2016. Mycosins are required for the stabilization of the ESX-1 and ESX-5 type VII secretion membrane complexes. *MBio* 7, 1–11. doi:10.1128/mBio.01471-16
- Volkman, H.E., Clay, H., Beery, D., Chang, J.C.W., Sherman, D.R., Ramakrishnan, L., 2004. Tuberculous granuloma formation is enhanced by a mycobacterium virulence determinant. *PLoS Biol.* 2, 1946–1956. doi:10.1371/journal.pbio.0020367
- Weerdenburg, E.M., Abdallah, A.M., Rangkuti, F., El, A., Otto, T.D., Adroub, S.A., Molenaar, D., Ummels, R., Stempvoort, G. Van, Sar, A.M. Van Der, Ali, S., 2015. Genome-Wide Transposon Mutagenesis indicates that *Mycobacterium marinum* customizes its virulence mechanisms for survival and replication in different hosts 83, 1778–1788. doi:10.1128/IAI.03050-14
- White, R.M., Sessa, A., Burke, C., Bowman, T., Ceol, C., Bourque, C., Dovey, M., Goessling, W., Burns, E., Zon, L.I., 2008. Transparent adult zebrafish as a tool for in vivo transplantation analysis. *Cell Stem Cell* 2, 183–189.
- World Health Organization, 2017. Global Tuberculosis Report 2017, WHO. doi:WHO/HTM/TB/2017.23